

REPORT DOCUMENTATION PAGE				Form Approved OMB NO. 0704-0188	
<p>The public reporting burden for this collection of information is estimated to average 1 hour per response, including the time for reviewing instructions, searching existing data sources, gathering and maintaining the data needed, and completing and reviewing the collection of information. Send comments regarding this burden estimate or any other aspect of this collection of information, including suggestions for reducing this burden, to Washington Headquarters Services, Directorate for Information Operations and Reports, 1215 Jefferson Davis Highway, Suite 1204, Arlington VA, 22202-4302. Respondents should be aware that notwithstanding any other provision of law, no person shall be subject to any penalty for failing to comply with a collection of information if it does not display a currently valid OMB control number.</p> <p>PLEASE DO NOT RETURN YOUR FORM TO THE ABOVE ADDRESS.</p>					
1. REPORT DATE (DD-MM-YYYY) 18-08-2009		2. REPORT TYPE Final Report		3. DATES COVERED (From - To) 13-Aug-2008 - 12-May-2009	
4. TITLE AND SUBTITLE CHARACTERIZATION OF NEAR-SURFACE MOISTURE DYNAMICS USING HYDROLOGIC MODEL-BASED INTERPRETATION OF GPR DATA				5a. CONTRACT NUMBER W911NF-08-1-0370	
				5b. GRANT NUMBER	
				5c. PROGRAM ELEMENT NUMBER 611102	
6. AUTHORS Stephen Moysey				5d. PROJECT NUMBER	
				5e. TASK NUMBER	
				5f. WORK UNIT NUMBER	
7. PERFORMING ORGANIZATION NAMES AND ADDRESSES Clemson University Office of Sponsored Programs 300 Brackett Hall Clemson, SC 29634 -5702				8. PERFORMING ORGANIZATION REPORT NUMBER	
9. SPONSORING/MONITORING AGENCY NAME(S) AND ADDRESS(ES) U.S. Army Research Office P.O. Box 12211 Research Triangle Park, NC 27709-2211				10. SPONSOR/MONITOR'S ACRONYM(S) ARO	
				11. SPONSOR/MONITOR'S REPORT NUMBER(S) 54969-EV-II.1	
12. DISTRIBUTION AVAILABILITY STATEMENT Approved for public release; distribution unlimited					
13. SUPPLEMENTARY NOTES The views, opinions and/or findings contained in this report are those of the author(s) and should not be construed as an official Department of the Army position, policy or decision, unless so designated by other documentation.					
14. ABSTRACT The objective of this project was to test whether transient GPR data provide useful information for constraining hydrologic processes in the vadose zone and evaluate alternative methods for hydrologic model calibration using this data. Modeling studies compared sequential and coupled inversion strategies using GPR data as a constraint on unsaturated hydraulic parameters. The coupled inversion approach, where hydrologic and geophysical models are linked together into a single forward model, was found to be an effective strategy for estimation of the flow					
15. SUBJECT TERMS GPR, unsaturated flow, vadose zone, calibration					
16. SECURITY CLASSIFICATION OF:			17. LIMITATION OF ABSTRACT SAR	18. NUMBER OF PAGES	19a. NAME OF RESPONSIBLE PERSON Stephen Moysey
a. REPORT U	b. ABSTRACT U	c. THIS PAGE U			19b. TELEPHONE NUMBER 864-656-0919

TABLE OF CONTENTS

PROBLEM STATEMENT.....	2
SUMMARY OF RESULTS.....	3
A. Numerical Comparison of Sequential and Coupled Inversion Schemes.....	3
B. Laboratory Investigation of GPR Response to Infiltration.....	4
C. Coherency Analysis of GPR Data for the Estimation of Hydrologic Parameters	5
D. Field Observations of GPR Response to Infiltration.....	7
PROJECT CONCLUSIONS.....	8
BIBLIORAPHY.....	9

LIST OF APPENDIXES

FINAL TECHNICAL REPORT.....	12
-----------------------------	----

LIST OF FIGURES

Figure 1: Observed and estimated GPR response in lab-scale studies.....	4
Figure 2: Signal power calculated along hydrologic trajectories.....	6
Figure 3: GPR data collected before and after a field-scale infiltration test.....	7

LIST OF TABLES

Table 1: Comparison of True Hydrologic Parameters to Estimates Obtained with Sequential and Coupled Inversion.....	3
---	---

PROBLEM STATEMENT

This research project investigated whether hydrologic model-based interpretation of transient GPR (ground-penetrating radar) data, the ground wave in particular, can lead to improved characterization of soil water dynamics. The strong dependence of the high-frequency dielectric permittivity of a soil on water content has made electromagnetic measurements (e.g., time domain reflectometry (TDR), ground-penetrating radar (GPR), and satellite radars) popular tools for monitoring near surface moisture conditions [e.g., Huisman et al., 2001; Entekhabi et al., 2004]. The GPR ground wave is of particular interest for providing high-resolution maps of near-surface water content at the catchment scale [Grote et al., 2003; Weihermuller et al., 2007]; such data would be invaluable for applications including understanding local rainfall-runoff and infiltration processes as well as calibrating satellite-based radar measurements for real-time monitoring of regional moisture conditions. A limitation of current interpretation techniques, however, is the assumption that the effective permittivity derived from a GPR measurement can be used to estimate the average water content of a soil, which can subsequently be used to interpret hydrologic processes. Previous studies have shown that problems like preferential sampling of high velocity zones by EM waves [Galagedara et al., 2005a,b; Moysey and Knight, 2004] and dispersive wave guides resulting from the infiltration of water [e.g., van der Kruk, 2006] can lead to systematic biases in water content estimates. This problem is compounded if the biased water contents are then used to calibrate non-linear unsaturated flow models. Following this sequential approach to geophysical data integration, i.e., estimating transient water contents with GPR and subsequently performing hydrologic analysis, may therefore lead to both inaccurate estimates of water content and poor predictions of unsaturated flow and transport. This research used modeling studies to evaluate whether a new, coupled approach to hydrogeophysical estimation of hydrologic parameters could outperform the sequential approach. The modeling was complimented by laboratory and field studies to assess whether the coupled approach could also be applied to real data.

SIGNIFICANCE OF THIS RESEARCH TO THE ARMY

Developing a methodology for the hydrologic analysis of GPR data to characterize soil moisture dynamics is of critical importance to the Army for several reasons, including understanding risks related to subsurface transport of Army-related contaminants, evaluating ground conditions affecting troop maneuvers under changing environmental conditions, and predicting surface runoff generation during rain events that can lead to flooding. Understanding the response of ground penetrating radar under dynamic soil moisture conditions is also of the utmost importance for improving the Army's ability to detect targets, such as landmines and buried ordnance, under field operating conditions.

SUMMARY OF MAJOR RESULTS

This summary provides a brief overview of work completed and results achieved in this research. A more detailed review of methods and analysis are given in the technical report in the appendix.

A. Numerical Comparison of Sequential and Coupled Inversion Schemes

The first problem addressed in this research was to assess the ability of sequential versus coupled inversion schemes to constrain the parameters of an infiltration model using GPR traveltimes data. Analytical models were selected for this analysis to allow for a Markov Chain Monte Carlo (MCMC) analysis to be performed. The Philip [1957] infiltration model was selected with a rectangular drainage model for redistribution, which results in 5 unknown hydrologic parameters controlling flow (sorptivity (S), saturated hydraulic conductivity (K_s), initial water content (θ_i), saturated water content (θ_s), shape parameter for $K(\theta)$ function (N)). This hydrologic model produces a sharp wetting front, which allows for calculation of GPR traveltimes (i.e., air wave, ground wave, reflected wave, refracted wave, and multiples) directly using ray theory. The MCMC analysis was performed using the Metropolis-Hastings algorithm to sample the posterior distribution of model parameters subject to the GPR data. In the case of sequential inversion GPR traveltimes data were used to estimate the depth of the wetting front and the water content above and below the wetting front, which were subsequently used to constrain the hydrologic model in a second inversion. In the coupled inversion GPR traveltimes were used to directly constrain the hydrologic model. Several different cases were investigated to evaluate the value of using different GPR arrivals as a data constraint, which included (i) the ground wave only, (ii) reflection from the wetting front only, and (iii) both the ground wave and reflected wave. A comparison of the true hydrologic parameters with those estimated by the sequential versus coupled approach is given in Table 1. Note that in all cases the traveltimes data were matched with a low degree of misfit.

Table 1: Comparison of hydrologic parameter estimates obtained with sequential and coupled inversion given different GPR traveltimes data as a constraint.

	TRUE VALUE	Ground Wave + Reflection		Ground Wave Only	
		Sequential	Coupled	Sequential	Coupled
θ_i	0.05	0.063	0.048	0.071	0.048
θ_s	0.35	0.343	0.349	0.257	0.351
K_s	0.72	0.560	0.785	0.004	0.836
S	0.98	0.919	0.986	3.573	0.995
N	2.00	0.985	4.736	3.328	2.336

For the case where both the ground wave and wetting front reflection are used as data constraints, there is a substantial amount of information available to capture the hydrologic behavior: the ground wave constrains the water content behind the wetting front while the reflection provides independent information on the velocity of the wetting front, which is dependent on both flux parameters (K and S) and storage potential (i.e., $\theta_s - \theta_i$). As a result, both the sequential and coupled inversion provide good estimates of the hydrologic model parameters, with the exception of N (Table 1). In contrast, when only the ground wave is used as a constraint, the independent information on the wetting front movement is lost. The sequential inversion therefore yields large uncertainty in both the wetting front depth and initial water content, which translates into poor estimates of the hydrologic model parameters (Table 1). The coupled inversion, on the other hand, continues to provide excellent estimates of the hydrologic model parameters (Table 1). This is because the hydrologic model provides an *additional*

constraint beyond the available geophysical data – both the traveltime data and the laws of hydrology must be honored at the same time in this inversion scheme. In this way the hydrologic model acts as a physically-based regularization to stabilize the inversion and provide accurate parameter estimates.

Conclusions: This part of the study illustrated that the coupled inversion scheme can significantly outperform sequential inversion for estimating unsaturated flow parameters.

B. Laboratory Investigation of GPR Response to Infiltration

The second part of this study evaluated the response of GPR to infiltration events using empirical data. To this end an irrigation system was developed that could provide a specified flux of water to the upper boundary of a sand box while coincidentally monitoring the infiltration event with GPR. The antennas were kept at a fixed location, but sampled continuously during the experiment. In the experiments, the flux applied to the upper boundary was varied as shown in Figure 1d to create multiple periods of transient and pseudo-steady state conditions. Water content sensors were located in the upper portion of the box (~5.5cm depth) and lower portion of the box (~45cm) to independently monitor moisture changes during the experiment.

The GPR data obtained using 900MHz antennas are shown in Figure 1a. Arrivals related to the ground wave and reflections originating from the bottom of the tank are clearly seen in the data. Also apparent are reflections related to wetting fronts resulting from both the initiation of flow at early times and from the first change in flux after 43 minutes from the start of the experiment. Subsequent wetting fronts at

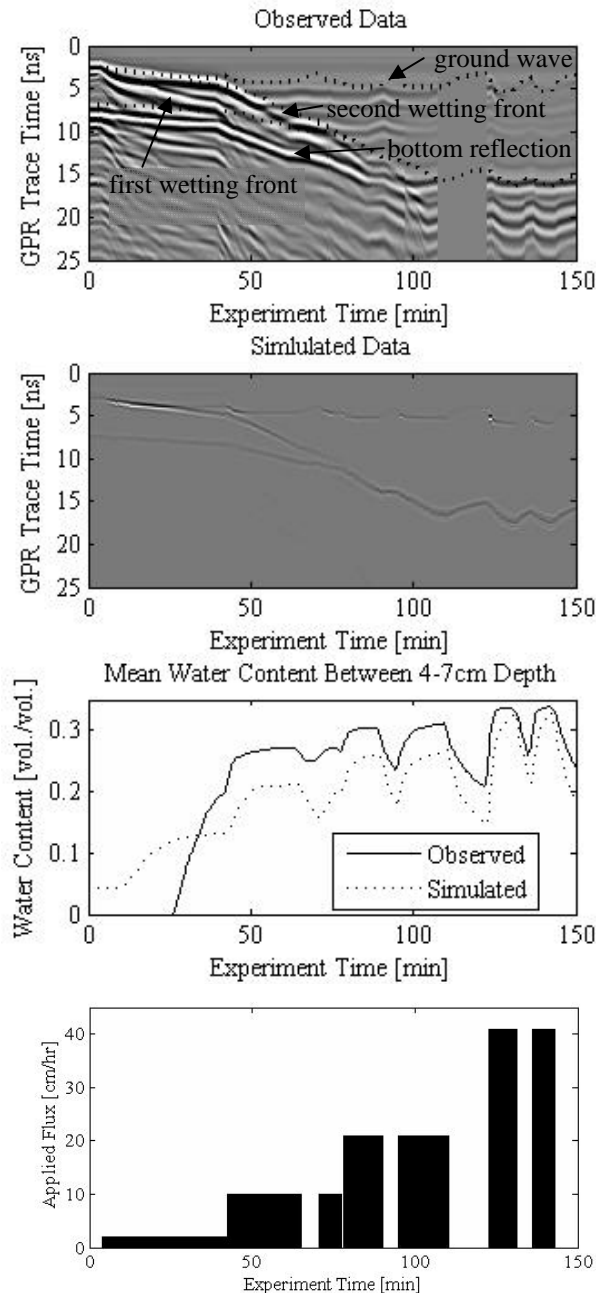


Figure 1: (a) Observed GPR response during infiltration event, dotted line shows comparison to arrival times in simulated data; (b) simulated GPR response based on lab measurements of hydraulic parameters, (c) average observed and simulated water content between 4-7cm depth, (d) water application schedule.

later times appear to have low amplitude given that the soil is already significantly wetted. The patterns observed in the data are in good agreement with the water content trends observed using the soil moisture probes (Figure 1c). Similar results were observed using 450MHz antennas except that the separation between the ground wave and reflections from the wetting front occurred at later times due to the lower frequency. As a result, it was more difficult to discriminate the wetting front reflections in that data.

To evaluate the empirical data, simulations of the GPR response were performed using the flow model HYDRUS-1D [Simunek et al., 2008] and a MATLAB based 2D GPR simulator created by Irving and Knight [2006]. The flow was simulated using the known boundary conditions, i.e., the applied flux in Figure 1d at the upper boundary and a seepage face condition on the lower boundary. The Mualem-van Genuchten model was to fit observed data for the unsaturated hydraulic conductivity and pressure-saturation function. The resulting predicted GPR response is shown in Figure 1b and predicted water content near the moisture probes in Figure 1c. The match between the simulated GPR response and the observed data is excellent given that the model prediction is based on independent samples and not calibration to the observed response. The ground wave, second wetting front, and bottom reflection are all clearly visible. An exception is the reflection from the first wetting front, which can be found in the simulated data but has much lower amplitude than in the empirical response. The traveltime for each of the main arrivals in the simulated data are plotted overtop of the empirical data in Figure 1a to provide a direct comparison between the results. It is apparent that there is generally a good match except during the period between 50-75 minutes where the simulated traveltimes are less than the observed response. The discrepancy between the observed and simulated water content can be explained by the underestimation of observed water content by the simulations in the near surface during this period (Figure 1c).

Conclusions: GPR is highly sensitive to infiltration processes showing strong pattern responses originating from the ground wave, reflections from wetting fronts, and subsurface heterogeneities (i.e., the tank bottom in this case). These responses form trajectories in the hydrologic data that are characteristic of hydrologic processes (e.g., soil wetting/drying). Current simulation tools are sufficient to represent the GPR response to infiltration under uniform flow in homogeneous soils.

C. Coherency Analysis of GPR Data for the Estimation of Hydrologic Parameters

A challenge that was identified in this research is that the MCMC approach to estimating hydrologic parameters from GPR data discussed above will likely be difficult to generalize for arbitrary hydrologic conditions. This is because models with a sharp wetting front, such as the Philip [1957] model, are limited to fairly simple hydrologic scenarios such as homogeneous soils with uniform initial water content and simple boundary conditions (i.e., fixed head or flux). Though in some cases these models are appropriate and the approach discussed in Section A can be applied, we found that simplified models are not always able to provide reliable simulations of water content for variable flux boundaries, such as that shown in Figure 1, given arbitrary soil parameters. As a result, numerical models for flow must be used to simulate water content under more general conditions. In this case, a sharp wetting front may not be defined and ray tracing or full numerical solutions to Maxwell's equations need to be used to simulate GPR responses. The increased computational burden could become a limiting factor for the computationally intensive MCMC techniques. To address this problem, a new approach for estimating

hydrologic properties that makes use of the trajectories observed in Figure 1 was hypothesized and investigated as a computationally efficient means for determining unsaturated flow parameters under arbitrary conditions. The approach is conceptually similar to normal moveout methods used to estimate wave velocity [e.g., Fisher et al., 1992].

A common method for analyzing multi-offset GPR data is to calculate a measure of coherency along the hyperbolic trajectory, i.e., normal moveout, describing the change of traveltimes with antenna offset as a function of EM wave velocity [Neidell and Taner, 1971]. This method works because the shape of the normal moveout trajectory is directly related to the wave velocity. The velocity that creates a trajectory through the data along which the similarity between the traces is maximized (i.e., traces constructively interfere when the normal moveout effect is taken into account) is likely the true velocity.

In the same way, it was speculated in this research that GPR data can be analyzed by calculating coherence measures along hydrologically defined trajectories (e.g., Figure 1) to determine hydrologic parameters controlling flow. In this work semblance and the signal power for data windows following the trajectories were used as measures of coherency. A key problem, however, is to define the hydrologic trajectories in a computationally efficient manner. For situations where a model with a sharp wetting front can be used this is easily accomplished using ray-based calculations. However, for arbitrary hydrologic scenarios an alternative method is proposed for finding the trajectories using GPR reflection coefficients. First, water contents are calculated with a numerical simulator (i.e., HYDRUS-1D) as a function of time and depth during the infiltration event, which can then be transformed to transient dielectric constant profiles. Converting the dielectric constants to velocity allows for the reflection coefficients to be mapped as a function of GPR arrival time. The reflection coefficients are then filtered to identify discrete arrivals that form hydrologic trajectories that are dependent on the initial unsaturated flow parameters (and boundary conditions) used to drive the infiltration model. The coherency of GPR data along the trajectories can then be evaluated by extracting the appropriate data from the observed GPR response. Therefore, the underlying hypothesis of the approach is that the true hydrologic parameters will produce trajectories that maximize the coherence of the GPR data.

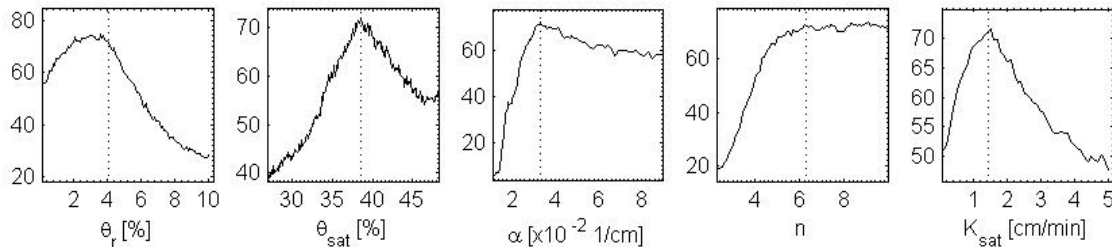


Figure 2: Signal power along the hydrologic trajectories as a function of the parameters for the Mualem-van Genuchten model. The dashed vertical line indicates the value of the true parameter. The maximum signal coherence is captured near the true parameter value except for the n parameter which does not appear to have a unique maximum.

An initial step toward testing this hypothesis was completed by performing a sensitivity analysis using the data shown in Figure 1b. Figure 2 shows the total signal power in the GPR data as a function of each of the hydrologic parameters. The result suggests that coherency of the signal is maximized by following a trajectory in the GPR data that is based on the true unsaturated flow parameters. The single major exception is the n parameter of the van

Genuchten model for the water retention curve, which is consistent with the result found in Section A where the coupled inversion of traveltime data provided a poor constraint on the shape parameter (N) of the unsaturated hydraulic conductivity function.

Conclusions: Analysis of signal coherency along hydrologic trajectories in GPR data could provide a means to optimize hydrologic model parameters with minimal computational effort.

D. Field Observations of GPR Response to Infiltration

Field-scale experiments were conducted to perform an exploratory investigation of transient GPR responses during infiltration in heterogeneous soils. In these experiments, we used a sprinkler system to irrigate an approximately 10m x 5m region of a silty-sand soil. GPR was profiled across the site at multiple times during the infiltration experiment. The GPR was profiled between fixed stations, but due to an inability to integrate real-time positioning information with our current GPR system and the discontinuation of odometer wheel triggering devices by the manufacturer of our radar, we were unable to precisely position the data. Instead, we attempted to consistently move the antennas at a constant velocity across the site – introducing the potential for positioning errors. Despite the possible positioning errors, Figure 3 illustrates significant shifts in the arrival time of the ground wave and different reflections across the site as a result of the infiltration event. In some areas, there is a change in the character of the GPR image, but it is currently unclear whether this is an effect resulting from the water infiltration or errors in positioning the antennas.

Conclusions: Shifts in GPR responses are likely to be clearly observable in field data. In this study we found that improved instrumentation for the positioning of the GPR antennas is needed to improve the data quality to allow for calibration of hydrologic models with GPR in the field.

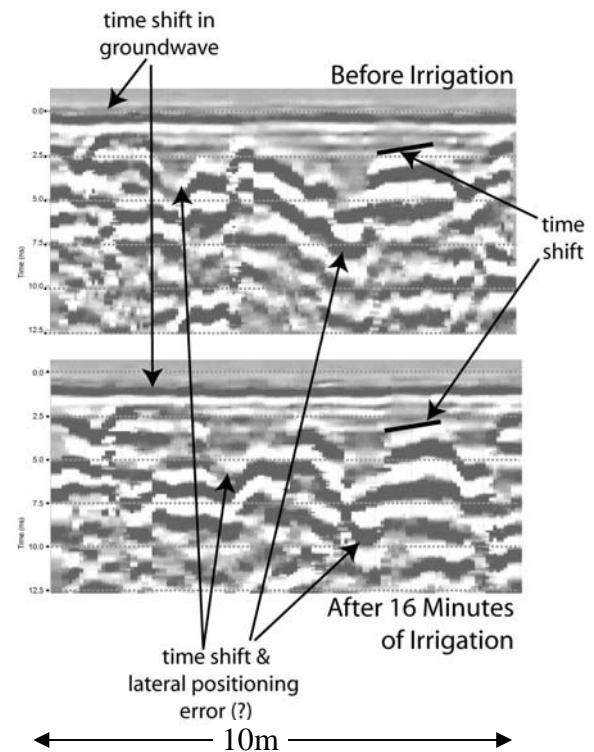


Figure 3: Two 10m transects of GPR data collected during a field infiltration experiment. The upper image shows the data collected prior to the start of the irrigation sprinklers. The bottom image shows the same transect profiled after 16 minutes of water application to the site. Note the shift in the groundwave and other reflections is a result of increased water content (decreased wave velocity) of the soils.

PROJECT CONCLUSIONS

This short term research project has demonstrated the potential of GPR for constraining the parameters of unsaturated flow models using the coupled approach to hydrogeophysical estimation. This is particularly true when GPR data contain insufficient information to independently constrain the hydrologic model. In this case, the coupled approach allows the hydrologic model to regularize the inversion and produce reliable estimates of hydrologic parameters. Stochastic calibration of models using traveltime data was shown to be effective for simple flow scenarios. Coherency analysis along hydrologic trajectories, a new methodology that was developed as a result of this research, shows promise for identifying hydrologic model parameters for more complicated flow scenarios. The behavior of the ground wave during infiltration was one particular point of interest in this research. While it was shown that the ground wave response is sensitive to flow processes, this research suggests that reflection data provide additional information on the rate of flow and can be readily included in model calibration algorithms. Therefore, it is recommended that all GPR arrivals be used to calibrate hydrologic models when possible.

BIBLIOGRAPHY

- Du, S., 1996, *Determination of water content in the subsurface with the ground wave of ground penetrating radar*, PhD Thesis, Ludwig-Maximilians-Universitat.
- Du, S., and P. Rummel, 1994, Reconnaissance studies of moisture in the subsurface with GPR: *Proceedings of the 5th International Conference on Ground Penetrating Radar*, University of Waterloo, 1241-1248.
- Entekhabi, D., E.G. Njoku, P. Houser, M. Spencer, T. Doiron, Y. Kim, J. Smith, R. Girard, S. Belair, W. Crow, T.J. Jackson, Y.H. Kerr, J.S. Kimball, R. Koster, K.C. McDonald, P.E. O'Neill, T. Pultz, S.W. Running, J. Shi, E. Wood, and J. vanZyl, 2004, The hydrosphere state (Hydros) satellite mission: an Earth system Pathfinder for global mapping of soil moisture and land freeze/thaw, *IEEE Transactions on Geoscience and Remote Sensing*, 42(10), 2184-2195.
- Fisher, E., G.A. McMechan, and A.P. Annan, 1992, Acquisition and processing of wide-aperture ground-penetrating radar data, *Geophysics*, 57:495-504.
- Fowler, D.E. and S.M. Moysey, 2007, Direct estimation of hydraulic conductivity using integrated inversion of resistivity data during a tracer test, *EOS Trans. AGU*, 88(52), Fall Meet. Suppl., Abstract H23A-1014.
- Galagedara, L.W., G.W. Parkin, J.D. Redman, P. von Bertoldi, A.L. Endres, 2005a, Field studies of the GPR ground wave method for estimating soil water content during irrigation and drainage, *Journal of Hydrology*, 301, 182-197.
- Galagedara, L.W., J.D. Redman, G.W. Parkin, A.P. Annan, and A.L. Endres, 2005b, Numerical modeling of GPR to determine the direct ground wave sampling depth, *Vadose Zone Journal*, 4, 1096-1106.
- Garambois, S., P. Senechal, and H. Perroud, 2002, On the use of combined geophysical methods to assess water content and water conductivity of near-surface formations, *Journal of Hydrology*, 259:32-48.
- Greaves, R.J., D.P. Lesmes, J.M. Lee, M.N. Toksoz, 1996, Velocity variations and water content estimated from multi-offset, ground-penetrating radar, *Geophysics*, 61(3):683-695.
- Grote, K., S.S. Hubbard, Y. Rubin, 2003, Field-scale estimation of volumetric water content using ground-penetrating radar ground wave techniques, *Water Resources Research*, 39(11), 1321, doi: 10.1029/2003WR002045.
- Hinnell, A.C., T.P.A. Ferre, J.A. Vrugt, S. Moysey, J.A. Huisman, and M.B. Kowalsky, 2008, submitted to *Water Resources Research*.
- Huisman, J.A., C. Sperl, W. Bouten, and J.M. Verstraten, 2001, Soil water content measurements at different scales: Accuracy of time domain reflectometry and ground-penetrating radar, *Journal of Hydrology*, 245, 48-58.
- Huisman, J.A., S.S. Hubbard, J.D. Redman, and A.P. Annan, 2003, Measuring soil water content with ground penetrating radar: A review, *Vadose Zone Journal*, 2, 476-491.
- Irving, J.D., and R.J. Knight, 2006, Numerical modeling of ground-penetrating radar in 2-D using MATLAB, *Computers & Geosciences*, 32:1247-1258.

- Jury, W. A. and R. Horton, *Soil Physics: Sixth Edition*, Wiley, New York, 2004.
- Klysz G., J.P. Balayssac, 2007, Determination of volumetric water content of concrete using ground-penetrating radar, *Cement and Concrete Research*, 37(8),1164-1171.
- Kowalsky, M.B., S. Finsterle, J. Peterson, S. Hubbard, Y. Rubin, E. Majer, A. Ward and G. Gee (2005), Estimation of field-scale soil hydraulic and dielectric parameters through joint inversion of GPR and hydrological data, *Water Resources Research*, 41(11), W11425, doi:10.1029/2005WR004237.
- Lambot, S., E.C. Slob, M. Vanclooster, and H. Vereecken, 2006, Closed loop GPR data inversion for soil hydraulic and electric property determination, *Geophysical Research Letters*, 33, L21405, doi:10.1029/2006GL027906.
- Menke, W., 1984, *Geophysical Data Analysis: Discrete Inverse Theory*, Elsevier, New York.
- Moysey, S., and R.J. Knight, 2004, Modeling the field-scale relationship between dielectric constant and water content in heterogeneous systems, *Water Resources Research*, 40, W03510, doi:10.1029/2003WR002589.
- Moysey, S.M., K. Singha, and R.J. Knight, 2005, A framework for inferring field-scale rock physics relationships through numerical simulation, *Geophysical Research Letters*, 32, DOI 10.1029/2004GRL022152.
- Moysey, S., R.J. Knight, and K. Singha, 2006, Relating geophysical and hydrologic properties using field-scale rock physics, *Proceedings CMWR XVI – Computational Methods in Water Resources*, Copenhagen, Denmark, 8p.
- Moysey, S.M., D.E. Fowler, and T. Sicilia, 2007, Impact of integrated versus sequential data fusion on hydrologic predictions, *EOS Trans. AGU*, 88(52), Fall Meet. Suppl., Abstract H41H-03.
- Neal, A., 2004, Ground-penetrating radar and its use in sedimentology: principles, problems and progress, *Earth-Science Reviews*, 66:261-330.
- Neidell, N.S., and M.T. Taner, 1971, Semblance and other coherency measures for multichannel data, *Geophysics*, 36(3):482-497.
- Philip, J. R., 1957, The theory of infiltration : 4. Sorptivity and algebraic infiltration equations, *Soil Science*, 84(3), 257-264.
- Rucker, D.F., and T.P.A. Ferré, 2004, Parameter estimation for soil hydraulic properties using zero-offset borehole radar: Analytical method, *Soil Science Society of America Journal*, 68, 1560–1567, 2004.
- Sicilia, G.T. and S.M. Moysey, 2007, Comparison of hydrologic parameter estimates using sequential and integrated data fusion during a GPR monitored infiltration event, *EOS Trans. AGU*, 88(52), Fall Meet. Suppl., Abstract H23A-1016.
- Simunek, J., M.Th. van Genuchten, and M. Sejna, 2008, Development and applications of the HYDRUS and STANMOD software packages and related codes, 7:587-600.
- Singha, K. and S. Moysey, S., 2006, Accounting for spatially variable resolution in electrical resistivity tomography through field-scale rock physics relations, *Geophysics*, 71(4), A25-A28, dio:10.1190/1.2209753.

- Singha, K., F.D. Day-Lewis, and S. Moysey, 2007, Accounting for tomographic resolution in estimating hydrologic properties from geophysical data, in *Subsurface Hydrology: Data Integration for Properties and Processes*, eds. D.W. Hyndman, F.D. Day-Lewis, and K. Singha, American Geophysical Union, Geophysical Monograph Series, Volume 171, doi:10.1029/170GM01, p.227-242.
- Strobbia, C., and G. Cassiani, 2007, Multilayer ground-penetrating radar guided waves in shallow soil layers for estimating soil water content, *Geophysics*, 72(4), J17-J29.
- Topp, G.C., J.L. Davis, and A.P. Annan, 1980, Electromagnetic determination of soil water content: Measurements in coaxial transmission lines, *Water Resources Research*, 16(3), 574-582.
- van der Kruk, J., 2006, Properties of surface waveguides derived from inversion of fundamental and higher mode dispersive GPR data, *IEEE Trans. Geosc. Rem. Sens.*, 44(10):2908-2915.
- van Overmeeren, R.A., S.V. Sariowan, and J.C. Gehrels, 1997, Ground penetrating radar for determining volumetric soil water content: Results of comparative measurements at two test sites, *Journal of Hydrology*, 197, 316-338.
- Weihermuller L., J.A. Huisman, S. Lambot, M. Herbst, H. Vereecken, 2007, Mapping the spatial variation of soil water content at the field scale with different ground penetrating radar techniques, *Journal of Hydrology*, 340, 205-216, doi:10.1016/j.jhydrol.2007.04.013.
- Weiler, K., T. Steenhuis, J. Boll, and K.-J. Kung, 1998, Comparison of ground penetrating radar and time domain reflectometry as soil water sensors, *Soil Science Society of America Journal*, 62, 1237-1239.
- Yilmaz, O., 1987, Seismic data processing, SEG Investigations in Geophysics 2, Society of Exploration Geophysicists, Tulsa, OK.

APPENDIX

STIR: CHARACTERIZATION OF NEAR-SURFACE MOISTURE DYNAMICS USING HYDROLOGIC MODEL-BASED INTERPRETATION OF GPR DATA

ARO Project Number: 54969-EV-II

– FINAL TECHNICAL REPORT –

Abstract: This report provides a brief summary of activities and accomplishments completed under ARO Project Number 54969-EV-II. The main objective of this short-term research project was to test the hypothesis that the GPR ground wave provides useful information for constraining hydrologic processes in the vadose zone. To investigate this problem a series of modeling and empirical studies were performed. The modeling studies examined whether GPR data could be directly used to constrain unsaturated hydraulic parameters using different approaches to parameter estimation. The coupled inversion approach, where hydrologic and geophysical models are linked together into a single forward model, was found to be an effective strategy for estimation of the flow parameters. Empirical studies focus on both laboratory and field tests. Lab studies were performed in a sand tank with spatially uniform applied infiltration. The results of these tests showed excellent sensitivity of GPR to infiltration processes and support the conclusions from the modeling studies that GPR can constrain hydrologic processes. In practice, however, multiple arrivals should be used in interpretation since the ground wave arrival is obscured by the reflection caused by the wetting front at early times during infiltration events. Field tests were performed to determine if transient patterns in GPR data could be observed in a heterogeneous environment under non-uniform flow conditions. These tests showed promising evidence to qualitatively suggest that the methodology used in this work will be applicable to field operations. A new method for the analysis based on measuring coherency along hydrologic trajectories in GPR data was developed and shown to provide good sensitivity to the parameters of the Mualem-van Genuchten model of unsaturated soils.

1. Introduction

The hypothesis tested in this research is that hydrologic model-based interpretation of transient GPR (ground-penetrating radar) data, the ground wave in particular, can lead to improved characterization of soil water dynamics. The strong dependence of the high-frequency dielectric permittivity of a soil on water content has made electromagnetic measurements (e.g., time domain reflectometry (TDR), ground-penetrating radar (GPR), and satellite radars) popular tools for monitoring near surface moisture conditions [e.g., Huisman et al., 2001; Entekhabi et al., 2004]. The GPR ground wave is of particular interest for providing high-resolution maps of near-surface water content at the catchment scale [Grote et al., 2003; Weihermuller et al., 2007]; such data would be invaluable for applications including understanding local rainfall-runoff and infiltration processes as well as calibrating satellite-based radar measurements for real-time monitoring of regional moisture conditions. A limitation of current interpretation techniques, however, is the assumption that the effective permittivity derived from a GPR measurement can be used to estimate the average water content of a soil, which can subsequently be used to interpret hydrologic processes. Previous studies have shown that problems like preferential sampling of high velocity zones by EM waves can lead to systematic biases in water content estimates [Moysey and Knight, 2004]. This problem is compounded if the biased water contents

are then used to calibrate non-linear unsaturated flow models. Following this sequential approach to geophysical data integration, i.e., estimating transient water contents with GPR and subsequently performing hydrologic analysis, may therefore lead to both inaccurate estimates of water content and poor predictions of unsaturated flow and transport.

This study investigated a new methodology for characterizing the evolution of soil moisture using ground penetrating radar. A unique aspect of this study is that the GPR data (e.g., travel times) were directly linked to soil properties controlling infiltration (e.g., hydraulic conductivity) by coupling hydrologic process models with geophysical instrument models. We demonstrate this approach using numerical experiments. The sensitivity of GPR to transient infiltration processes was investigated empirically using 1D infiltration experiments performed in a laboratory sand tank. These experiments were used to verify that specific arrivals could be identified in the GPR data and to evaluate the sensitivity of the data to infiltration. Finally, we describe exploratory field experiments that were designed to investigate whether the proposed methodology could be applied to field studies.

2. Background

2.1 Estimation of water content using GPR

GPR data – the GPR ground wave in particular – has received increasing attention as a tool for mapping near surface water content variations [Du and Rummel, 1994; Du, 1996; van Overmeeren et al., 1997; Weiler et al., 1998; Grote et al., 2003; Huisman et al., 2001, 2003; Klys and Balayssac, 2007; Strobba and Cassiani, 2007; Weihermuller et al., 2007]. The ground wave is the portion of energy emitted from a GPR transmitter antenna that travels directly to the receiver antenna through the soil (Figure 1). The travel time between the transmitter and receiver can be identified in the radar data and used to determine the velocity of the EM wave, which is primarily related to the dielectric permittivity of the soil. In most soils,

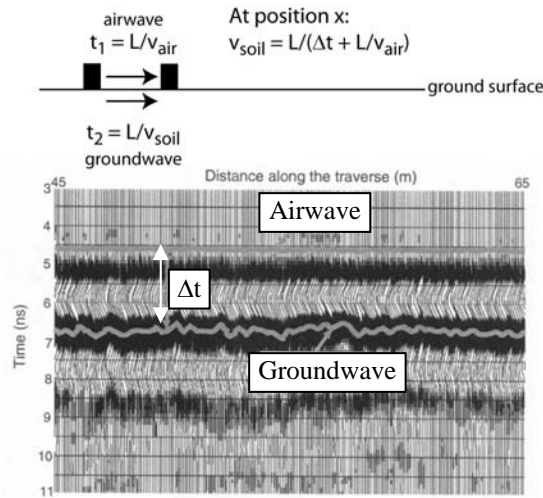
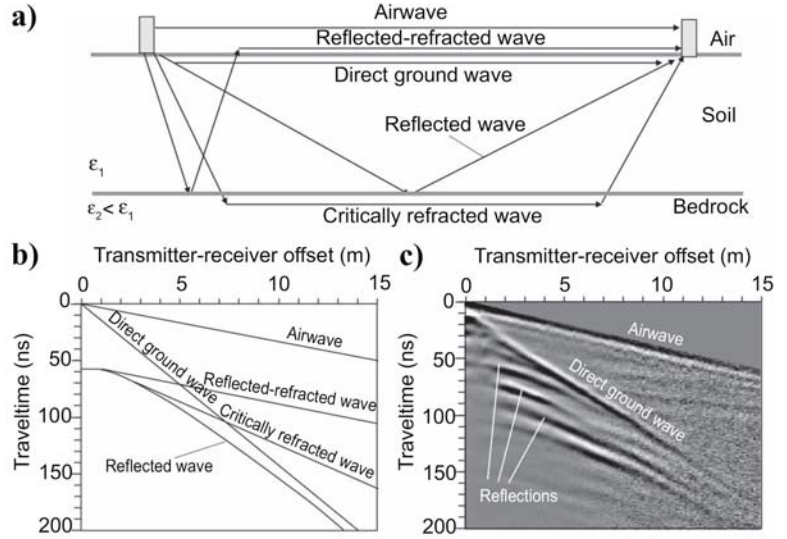


Figure 1: Near-surface water content variations can be identified from fluctuations in the arrival of the GPR ground wave. The constant-offset measurement geometry is shown above example data (after Grote et al., 2003).

dielectric permittivity is strongly dependent on water content [e.g., Topp et al., 1980; Huisman et al., 2001]. By keeping the transmitter and receiver antennas separated by a fixed spacing as they are moved across the ground surface it is possible to quickly map near-surface water contents over large regions [e.g., Grote et al., 2003].

In addition to the ground wave, however, multiple other arrivals are also produced as a result of alternate pathways transferring energy between source and receiver antennas (Figure 2). Strobba and Cassiani [2007] recently pointed out how refracted waves could also severely impact the interpretation of water content using the GPR ground wave. Refracted waves occur when energy follows a ray path that bypasses low-velocity zones, thereby potentially arriving at the receiver earlier than direct or reflected waves. Soil velocities can be significantly overestimated if the arrival of a refracted wave obscures the ground wave or is

Figure 2: (a) Possible ray paths for energy traveling between GPR transmitter and receiver antennas when a wet layer is present near the surface. (b) Expected arrival time for each ray path as a function of antenna separation. Note that the ground wave arrival may be obscured at small offsets by the air wave and at larger offsets by refracted waves. (c) An example of CMP data that can be used to optimize the transmitter-receiver survey to minimize wave interference for profiling studies. (From Strobba and Cassiani, 2007).



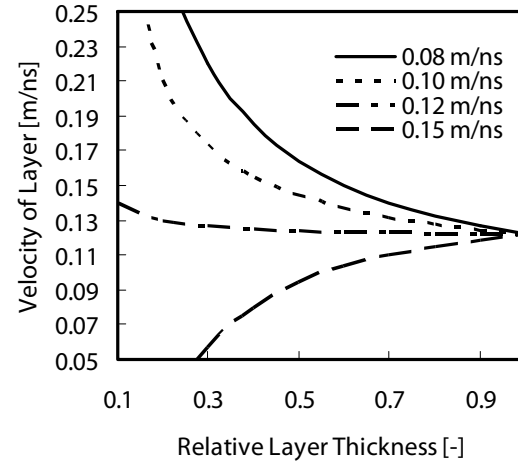
mistakenly identified as the ground wave. Given that infiltration events by nature generate slow (i.e., wet) zones overlying fast (i.e., dry) zones, refracted waves might be expected to be a common problem. This is a particularly serious issue for estimating water content from fixed offset profiles (of the type shown in Figure 1). When multi-offset profiles are collected, distinctive patterns in the data (e.g., Figure 2b) can be used to discriminate between different arrivals and thereby guide interpretation. However, van der Kruk [2006] recently discussed how low velocity layers, like infiltration fronts, can act as a dispersive wave guide that lead to a “shingling” effect in multi-offset GPR data; the implication being that incorrect velocities will be estimated even in this approach without special inverse procedures. These issues are significant problems for fixed offset GPR data. Discrimination based on the data alone is not possible and errors in the estimation of the ground wave velocity are likely to occur. In contrast, discrimination between alternate subsurface models can be effectively achieved when the field data are compared to the results of numerical simulations, even when interference from refracted waves occurs [e.g., Strobba and Cassiani, 2007] or, we hypothesize, when the wave guide effect is present.

Another significant challenge in using the ground wave to investigate soil water dynamics is that the support volume of the measurement is not well defined. Grote et al. [2003] cite half the Fresnel zone as the potential depth of investigation, thus making the sample volume dependent on measurement frequency, wave velocity in the soil, and antenna separation. In a numerical study Galagedara et al. [2005b] specifically investigated ground wave velocity in a material with a near surface wet or dry layer, i.e., scenarios typical of wetting and drying soils. They found that the depth of investigation was approximately 60% of the GPR wavelength, thus confirming the dependence on measurement frequency and soil velocity. More importantly, when the layer thickness was between ~ 0.25 – 0.6 of the GPR wavelength, they observed a nearly linear dependence of soil velocity on layer thickness. It is clear that with this type of simple linear mixing, i.e., $v_{\text{soil}} = f v_1 + (1-f) v_2$, it is straight forward to determine the apparent velocity of a soil (v_{soil}) if the depth of a wetting front (f) (relative to the GPR wavelength) is known along with the velocity (i.e., water content) within the wetted (v_1) and dry (v_2) zones. However, it is impossible to uniquely estimate the water content in the wetted zone without making

assumptions regarding the depth of the wetting front and initial water content (Figure 3). Thus the measurements of ground wave velocity may not lead to a good representation of moisture conditions in the very near surface environment (e.g., <10cm), which is the critical interface between the subsurface, land surface and atmosphere. This problem is evident in the empirical results of Galagedara et al. [2005a] where they found that a good match between GPR and TDR measurements during infiltration and drying events could only be obtained when the length of the TDR probes was similar to the GPR investigation depth.

The unknown support volume of the ground wave, interference from refractions, and preferential sampling of high velocity zones are all problems that can confound the estimation of water content from ground wave data. However, the effect of each of these issues can be readily accounted for using forward models describing GPR wave propagation. As a result, the hydrologic interpretation of ground wave data could be improved significantly if the analysis of the ground wave was performed by comparing observed transient field data with numerical simulations through inversion. In practice, however, even with the use of forward modeling, a priori information may be needed to provide an additional constraint that would allow investigation of subsurface dynamics during infiltration with GPR (e.g., as demonstrated by Figure 2). This research investigates whether this additional level of constraint provided by transient data can be imposed through the use of hydrologic models to generate physically possible subsurface realizations that can be used to drive GPR forward simulations.

Figure 3: Illustration of the non-unique nature of ground wave data for estimating the velocity and thickness of a near-surface layer given a simple linear mixing law. Every combination of parameters shown will produce an effective (i.e., ground wave) velocity of exactly 0.122 m/ns. Each line represents a different possible velocity for the region below the layer. Essentially any water content could be predicted in the near surface layer unless additional constraints on water content below the layer and layer thickness are given.



2.2 Hydrologic Model-Based Interpretation of Geophysical Data

The current state-of-the-art approach to integrating geophysical methods into hydrologic problems is a two-step process (Figure 4). First geophysical data are collected and analyzed to extract information about the distribution of geophysical state variables in the subsurface (e.g., extraction of dielectric permittivity from ground wave arrival times). Rock physics relationships

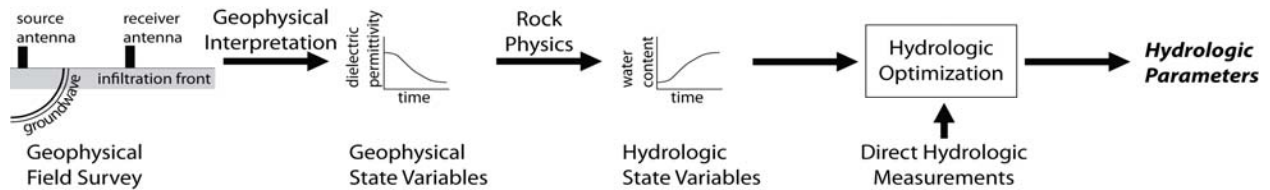


Figure 4: The current state-of-the-art integration of geophysical data into a hydrologic problem follows a sequential process where geophysical data are collected and analyzed to yield indirect estimates of hydrologic state variables (e.g., water content). In a subsequent analysis effort, these estimates may be used as data within an optimization scheme to calibrate the parameters of hydrologic models.

are used to convert these values to hydrologic state variables (e.g., water content), which may subsequently be used to constrain the parameters governing hydrologic process models.

A key limitation of this approach is that the resolution of geophysical data is often only sufficient to uniquely identify averages of subsurface properties (as demonstrated in Figure 3). The inverse problem is therefore typically mathematically stabilized (i.e., regularized) using a priori information, such as constraints on spatial continuity of the geophysical properties [e.g., Menke, 1984]. Often times the choice of prior information is arbitrary, e.g., through the application of a smoothness constraint on the estimated model, rather than selected objectively based on observed data or readily identifiable laws. As a consequence, the rock physics conversion from geophysical to hydrologic properties at the field scale can be complicated, spatially variable, and dependent on both measurement geometry and subsurface properties [Moysey et al., 2005; Singha and Moysey, 2006; Singha et al., 2007]. Moysey et al. [2006] speculated that this non-uniqueness problem (and therefore the associated field-scale rock physics problem) could be overcome if the laws of hydrology are used to enforce a priori constraints on the distribution of geophysical state variables rather than making arbitrary choices about the spatial distribution of these properties.

Using hydrologic models to constrain the inversion of geophysical data (Figure 5) is a relatively new idea that has not yet received an extensive amount of attention [Rucker and Ferre, 2004; Kowalski et al., 2005; Lambot et al., 2006; Sicilia and Moysey, 2007; Fowler and Moysey, 2007; Moysey et al., 2007; Hinnell et al., 2008 (*submitted to WRR*)]. The approach initiates by selecting a set of test parameters to run a hydrologic model used to predict the spatial and temporal distribution of hydrologic state variables through time. Point-scale rock physics relationships, which are easier to define than field-scale rock physics relationships [Moysey et al., 2006], are used to transform the hydrologic state variables to geophysical properties. A geophysical instrument model is then used to replicate the actual experiment performed in the field. A poor comparison between the simulated and observed field data indicates a poor initial choice of parameters in the hydrologic model thereby leading to an update of these parameters. The model parameters are updated continuously until a good match between the simulated and observed geophysical data is obtained.

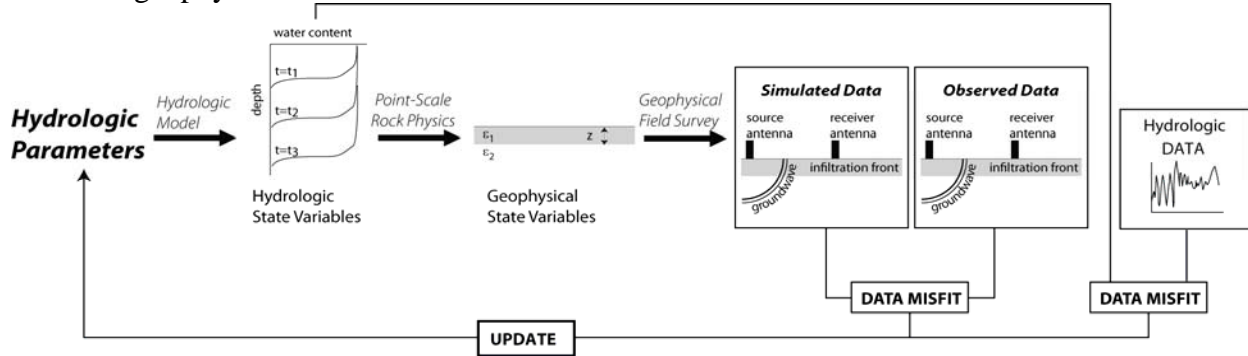
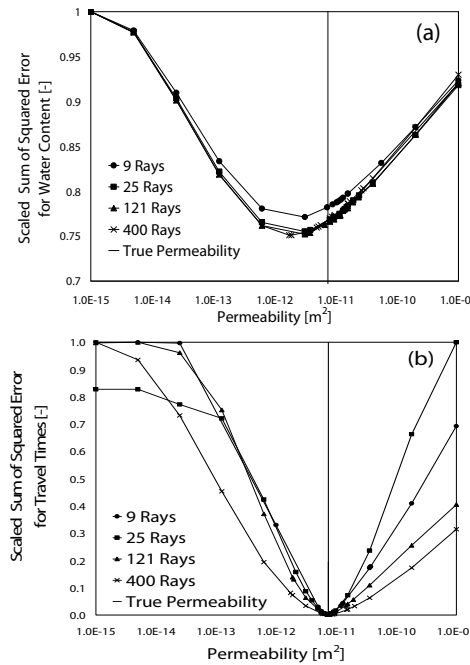


Figure 5: Coupling hydrologic process models with geophysical instrument models establishes a direct link between geophysical data and hydrologic parameters. This new approach to hydrogeophysical data integration avoids the geophysical inversion step and therefore does not impose arbitrary prior constraints on the geophysical properties. In this approach *a priori* constraints on the geophysical properties are automatically imposed by the physical laws built into the hydrologic model.

Note that in this procedure there is no geophysical interpretation step – the geophysical properties are only involved in forward models, not inverse models, so there is no need for the assumption of a priori constraints on these properties. Also, there is no restriction on the

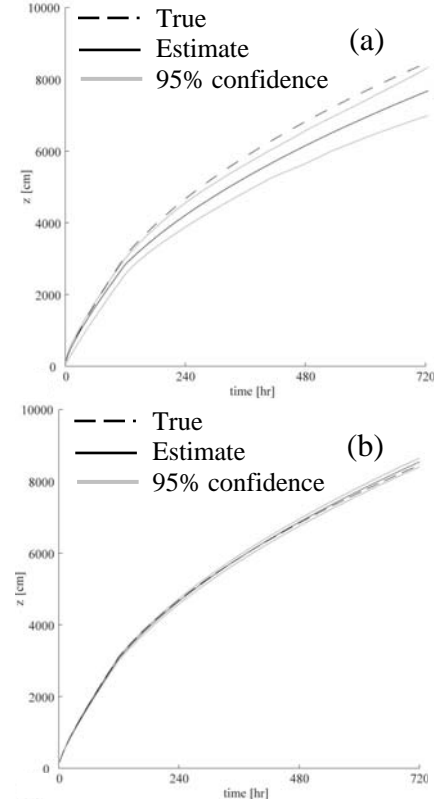
complexity of the geophysical data used in the inversion. For example, rather than extracting ground wave travel times from the GPR data, the comparisons between simulated and observed data could be made for the GPR amplitude record. As a result, interactions between different arrivals may be considered as an opportunity to identify and discriminate processes, rather than a problem that reduces data quality.

To date few studies have used the coupled interpretation approach to calibrate infiltration models using GPR data. Kowalski et al. [2005] illustrated that a coupled analysis could be used to estimate flow properties using cross-borehole GPR monitoring of an infiltration event. Lambot et al. [2006] performed a synthetic experiment to demonstrate that air-launched radar measurements could theoretically be used to constrain infiltration processes. Sicilia and Moysey [2007] performed the first comparative analysis of the sequential (Figure 4) and coupled (Figure 5) data integration methods. These authors investigated whether intrinsic permeability values could be constrained by monitoring an infiltration event with cross-borehole GPR. They found that the sequential analysis resulted in permeability estimates that consistently underestimated true values by an order of magnitude (Figure 6a). In contrast, the coupled analysis resulted in no permeability bias and overall produced much better fits between simulated and observed data (Figure 6b). Hinnell et al. [2008 (submitted to WRR)] present a synthetic study where surface-based electrical resistivity monitoring of 1D infiltration is used to estimate 5 different soil properties. These authors used an implementation of a Markov Chain Monte Carlo method to compare both the estimation accuracy and uncertainty resulting from the sequential versus coupled analysis strategies. Figure 7 shows predictions of the wetting front depth versus time based on the flow models calibrated with the resistivity measurements. Note that the data used in either case is identical; the only difference between the results is whether the sequential or coupled interpretation technique was used. These studies illustrate the potential performance improvement that can be gained by enforcing hydrologic constraints on the geophysical data.



←**Figure 6:** Comparison of objective functions for the estimation of permeability using (a) sequential and (b) coupled analyses of a GPR monitored infiltration test. Note that the sequential approach results in a bias in the estimate and higher data misfit than the coupled approach (Sicilia and Moysey, 2007).

→**Figure 7:** Predicted depth of an infiltration front using a model calibrated with resistivity data using (a) sequential and (b) coupled analyses. Note that the sequential approach yields much larger levels of prediction uncertainty, yet the true front still falls outside the 95% confidence bounds of the prediction. (Hinnell et al., 2008).



3. Overview of Methods and Results from this Research

This research investigated the use of GPR data for constraining hydrologic models using three approaches: (1) numerical modeling, (2) laboratory studies, and (3) field studies. The methods and results obtained from each of these is outlined below in the three following sections.

3.1 Numerical Modeling Study

3.1.1 Description of Model

The modeling in this study focused on comparing the sequential (Figure 4) and coupled (Figure 5) inversion approaches for estimating hydrologic properties from GPR data. The initial set of numerical experiments considered a scenario of 1D infiltration under zero ponding depth in a uniform soil with constant initial water content (θ_i). In this case, infiltration can be described using the Philip [1957] model where cumulative infiltration $I(t)$ at an arbitrary time t is related to the sorptivity (S) and saturated hydraulic conductivity (K_s) of the soil:

$$I(t) = St^{\frac{1}{2}} + K_s t \quad (1)$$

The wetting front z_{wf} in the Philip model is a sharp boundary such that the depth of the interface can be defined at any time by the storage capacity of the soil (i.e., $\theta_{wf} - \theta_i$) and cumulative infiltration:

$$z_{wf}(t) = \frac{I(t)}{\theta_{wf} - \theta_i} \quad (2)$$

where the water content above the wetting front is θ_{wf} , which is equal to the saturated water content θ_s throughout the infiltration period.

During the redistribution phase was modeled as a zero flux boundary and flow was assumed to be gravity driven. In this case, further migration of the wetting front must result from a decrease in storage, i.e., change of water content above the wetting front. We used a rectangular drainage model [e.g., Jury and Horton, 2004] to represent this process:

$$z_{wf} = Z_d \frac{\theta_{wf}(t_d) - \theta_i}{\theta_{wf}(t) - \theta_i} \quad (3)$$

where Z_d is the depth reached by the wetting front at the end of the infiltration period and t_d is the time at which infiltration ceased. Under gravity driven flow the flux q is controlled by the unsaturated hydraulic conductivity $K(\theta)$, i.e., $q = K(\theta)$. In this study, an exponential relationship was used for the unsaturated conductivity function:

$$\frac{K(\theta)}{K_s} = \left(\frac{\theta - \theta_i}{\theta_s - \theta_i} \right)^N \quad (4)$$

where θ is the water content at an arbitrary time t , θ_s is the water content at saturation, and N is a soil-specific parameter. The water content behind the wetting front at any time after the cessation of infiltration, i.e., $t - t_d$, will then be given by:

$$\theta_{wf}(t) = \left[\frac{NK_s}{L} (\theta_s - \theta_i)^{-(N+1)} (t - t_d) + \frac{1}{(\theta_s - \theta_i)^N} \right]^{-\frac{1}{N}} + \theta_i \quad (5)$$

Though this model is simple, it is also powerful. For example, Figure 8 compares the soil moisture distribution predicted by this model and the numerical solution of Richard's equation as simulated by the numerical model Hydrus1D. Though the details are slightly different, there is

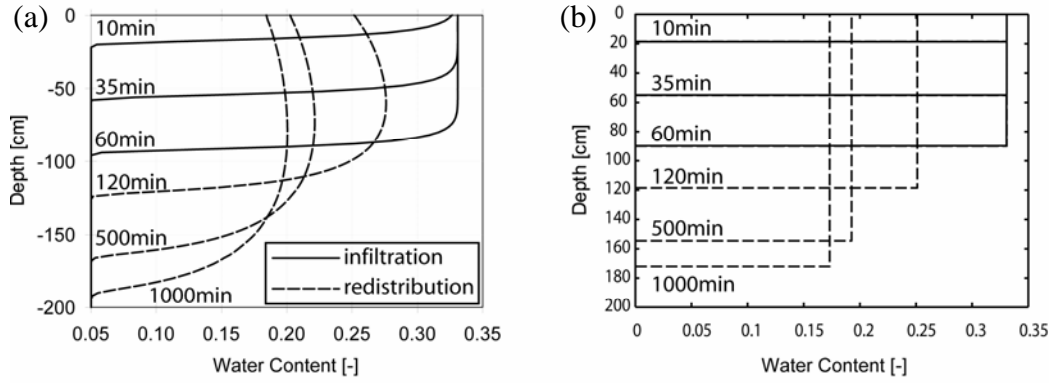


Figure 8: Comparison of the evolution of water content profiles during an infiltration event as determined by (a) solution of Richards' equation with Hydrus-1D and (b) the Philip infiltration and rectangular redistribution model. Although the details of the depth profiles are slightly different, the simple model captures the gross changes in water content that are likely to affect GPR measurements in a fraction of the computational time.

an excellent reproduction of the overall infiltration and redistribution process. Furthermore, the model used here can be used to simulate flow in a fraction of the time required to run a full numerical solution, thus is more appropriate for use in stochastic estimation algorithms; the simulation in Figure 8a required 18 seconds of computational time on a 1.73GHz desktop computer with 2GB of RAM, whereas the simulation in Figure 8b required only 0.01 seconds on the same computer.

The results shown in Figure 8 also emphasize the fact that the infiltration-redistribution model conceptualizes the subsurface as a time-variable, single layer system, i.e., the region behind the wetting front above a homogeneous background. This can therefore also be modeled as a single layer system for GPR where we have used Topp's equation to relate water content and dielectric constant [Topp et al., 1980]. Assuming a low-loss environment, the velocity of the EM wave is given by $v=c/\kappa^{0.5}$, where c is the speed of light and κ is the dielectric constant of the soil. The GPR travel time for various pathways can be calculated analytically for this single layer model using ray theory. For example, the travel time of the ground wave (T_g) would simply be $T_g = L/v_{gw}$, where L is the antenna separation and v_{wf} is the velocity of the EM wave behind the wetting front. Note that at late times, when the wetting front has passed the sampling depth of the ground wave v_{gw} would simply be the velocity of the soil behind the wetting front; before this time, however, the effective velocity will be an average of the velocities above and below the wetting front [e.g., Galagedara et al., 2005b]. Likewise, the travel time for a reflection from the wetting front would be given by $T_{wf} = 2 * ((L/2)^2 + z_{wf}^2)^{0.5} / v_{wf}$.

3.1.2 Simulation Details and Estimation Procedure

To compare the performance of the sequential and coupled inversion strategies, a numerical experiment was conducted where infiltration was simulated for 5 minutes followed by a 28.5 minute period of redistribution. The “true” soil properties used for this test are given in Table 1. The resulting water content distribution as a function of time is shown in Figure 9. The GPR travel times for the ground wave and reflection from the wetting front boundary are given in Figure 10; 1% random Gaussian noise was added to each travel time.

Table 1: Soil parameters used in the modeling study

θ_i [-]	θ_s [-]	K_s [m/day]	S [m/day ^{0.5}]	N [-]
0.05	0.35	0.72	0.98	2

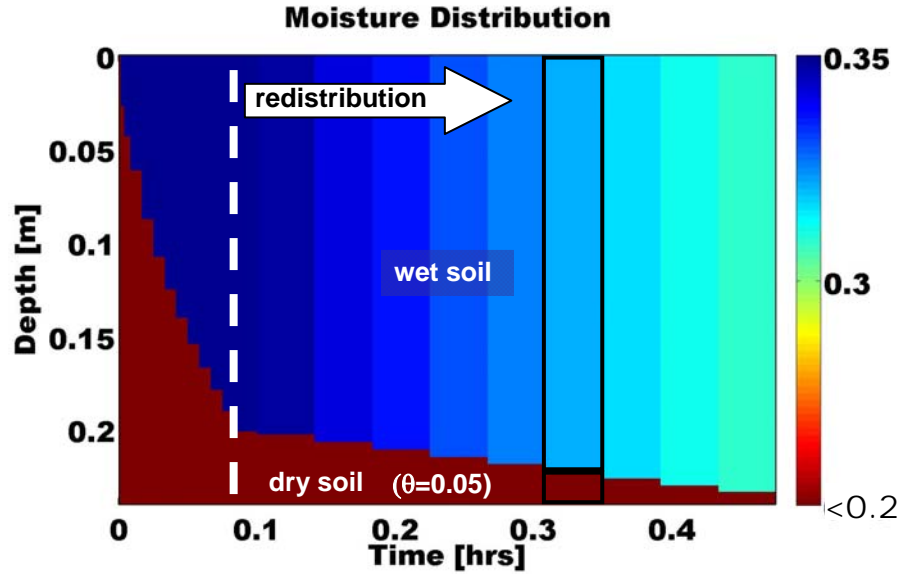


Figure 9: Position of the wetting front and water contents as a function of time during the simulated infiltration experiment.

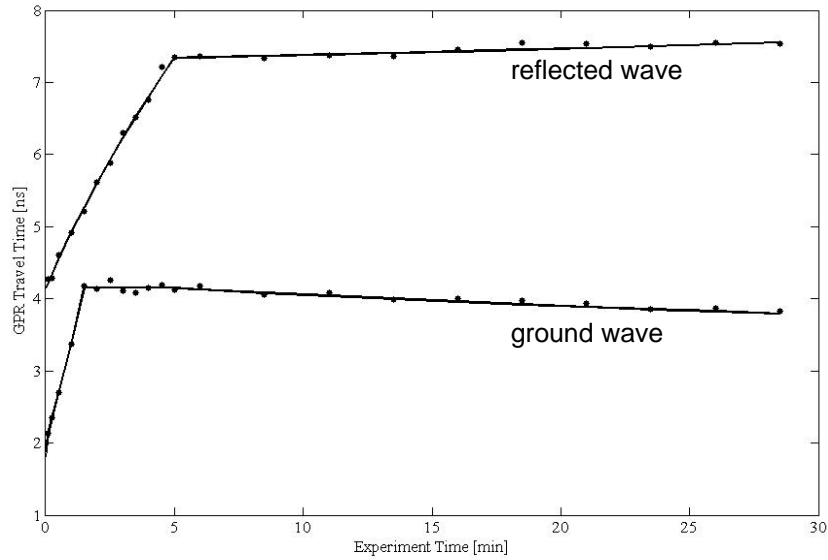


Figure 10: Travel times for the GPR ground wave and reflection from the wetting front during infiltration and redistribution. Random Gaussian noise (1%) was added to each travel time.

The noisy travel times in Figure 10 represent the data used to constrain the hydrologic parameters of the infiltration and redistribution model using both the sequential and coupled inversion. In the case of sequential inversion (Figure 4), the travel times were first used to estimate EM wave velocity above of the wetting front and the depth to the interface. The velocities were then converted to water contents and used as a constraint in a second optimization to determine the hydrologic properties. For the coupled inversion, in contrast, the travel times were used as a direct constraint on the hydrologic model using the approach outlined in Figure 5. In both cases, the Metropolis-Hastings algorithm was used to sample the posterior probability distribution of the model parameters. Gaussian distributions were assumed for the likelihood function in all cases and candidate distributions for parameters were limited to the ranges given in Table 2.

Table 2: Bounds and initial value of parameters used in Metropolis-Hastings algorithm

	Hydrologic Parameters					Geophysical Parameters		
	θ_i [-]	θ_s [-]	K_s [m/day]	S [m/day ^{0.5}]	N [-]	v_{wf} [m/ns]	v_i [m/ns]	z_{wf} [m]
Lower Bound	0	0.1	0	0	0	0	0.08	0
Upper Bound	0.2	0.6	5	5	5	0.1	0.18	1
Initial Value	0.01	0.3	1.5	0.5	1.5	0.05	0.18	0.5

3.1.3 Summary of Results

Using MCMC to sample the posterior distribution produces a collection of viable parameter sets. For the sequential inversion 10,000 sets of the three geophysical variables (velocity above and below the wetting front and depth to the wetting front) were generated with the Metropolis-Hastings algorithm at each observation time; the mean and standard deviation for each parameter are shown in Figure 12. For both the sequential and coupled inversion, the Metropolis-Hastings algorithm was used to sample 20,000 samples of the 5 hydrologic parameters (i.e., θ_i , θ_s , K_s , S , N); the mean and standard deviation of these results are given in Tables 3 and 4. For the sequential inversion this was accomplished by converting each set of velocities to water content using the low-loss relationship between velocity and dielectric constant ($\kappa = (0.3/v)^2$, where v is velocity in m/ns) and then applying the Topp equation [1980]. The resulting water contents were then used as data to constrain the hydrologic model. In contrast, the GPR traveltimes are used directly as a constraint on the hydrologic parameters for the linked hydrologic and geophysical model in the coupled inversion.

The fit of the GPR traveltimes using the sequential estimation approach is excellent as shown in Figure 11. Despite the excellent fit to the traveltime data, Figure 12 indicates an inability to reliably constrain the velocity below the wetting front. Regardless, the velocity above the wetting front and the depth to the front are estimated with reasonable accuracy. This is not surprising since for a 2 layer model the ground wave arrival provides a constraint on velocity above the wetting front and the reflected wave provides an independent constraint on the depth to the interface. However, there is also the potential for tradeoffs between layer thickness and apparent velocity above the wetting front as described in Figure 3. This effect is thought to be responsible for the “spikes” apparent in the velocity above the wetting front which are paired to similar spikes in wetting front depth – note that the traveltime data are still fit very well despite the inaccuracy of the velocity and depth estimate.

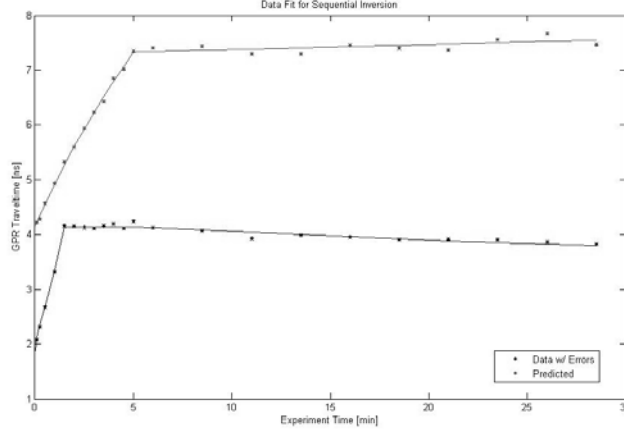


Figure 11: Fit of the GPR traveltime data using the sequential inversion.

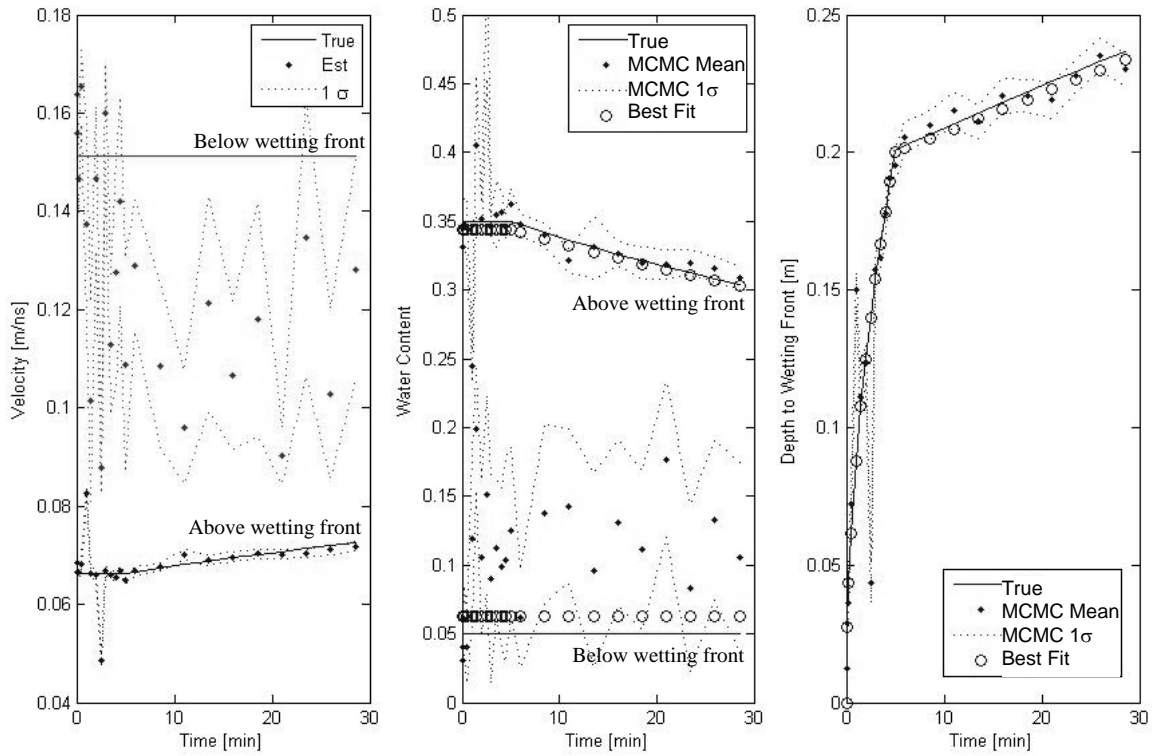


Figure 12: Sequential estimates of model parameters using MCMC at each time of the simulation – (a) velocity above and below the wetting front, (b) water content above and below the wetting front, (c) depth to the wetting front. Dots represent the mean of all parameter sets accepted using the Metropolis-Hastings algorithm and dashed lines represent 1σ . Open circles show the water content and wetting front depth predicted by the hydrologic parameter using the best fit (i.e., mean) parameters from Table 3. The solid lines show the true model response.

Table 3: Estimation results using GPR traveltimes from both the ground wave and wetting front reflection. Mean and standard deviation of the hydrologic parameters estimated from samples from the posterior distributions using MCMC.

	TRUE VALUE	SEQUENTIAL ESTIMATE		COUPLED ESTIMATE	
		Mean	σ	Mean	σ
θ_i	0.05	0.063	0.007	0.048	0.001
θ_s	0.35	0.343	0.003	0.349	0.001
K_s	0.72	0.560	0.073	0.785	0.056
S	0.98	0.919	0.026	0.986	0.007
N	2.00	0.985	0.378	4.736	0.165

The fit to the traveltime data for the coupled inversion is shown in Figure 13. The main difference from the sequential result is that the noise in the data are not fit, while the main trends are. This is a consequence of the fact that the coupled hydrogeophysical model provides a regularizing effect on the estimation – the noise in the data cannot be explained by the hydrologic model, thus cannot be fit by the coupled geophysical and hydrologic models. In other words, the coupled inversion is more stable and less sensitive to noise than the sequential inversion. The hydrologic response predicted by the best fit parameter estimates for the coupled inversion are given in Figure 14. The match between the true response and that predicted by the calibrated model is excellent.

The estimation procedure described above was repeated using only the ground wave traveltimes and again using only the traveltimes for the reflection from the wetting front; the results are given in Tables 4 and 5, respectively. When only the ground wave is used, the velocity of the upper layer is well constrained, but the constraint on the wetting front depth that had previously been provided by the reflection data is lost (compare Figure 12c to Figure 16c). The results of the sequential inversion suggest that knowing the water content of the upper layer alone is not sufficient to constrain the model parameters. In contrast, in the coupled inversion good estimates of the hydrologic parameters can still be achieved because the hydrologic model implicitly places an *additional constraint* of how the water contents in the upper layer are allowed to change through time. This extra information along with the ground wave data appears to be sufficient to constrain the behavior of the model (Figure 17). The contrast between the performance of the sequential and coupled inversion schemes in this example highlights the concept that the hydrologic model provides a physically based regularization on the inversion.

Table 4: Estimation results using GPR traveltimes from only the ground wave.

	TRUE VALUE	SEQUENTIAL ESTIMATE		COUPLED ESTIMATE	
		Mean	σ	Mean	σ
θ_i	0.05	0.071	0.005	0.048	0.001
θ_s	0.35	0.257	0.001	0.351	0.002
K_s	0.72	0.004	0.004	0.836	0.077
S	0.98	3.573	0.098	0.995	0.014
N	2.00	3.328	0.228	2.336	0.589

Table 5: Estimation results using GPR traveltimes from only the wetting front reflection.

	TRUE VALUE	SEQUENTIAL ESTIMATE		COUPLED ESTIMATE	
		Mean	σ	Mean	σ
θ_i	0.05	0.082	0.011	0.055	0.022
θ_s	0.35	0.297	0.015	0.349	0.003
K_s	0.72	0.102	0.093	0.696	0.152
S	0.98	0.624	0.061	0.964	0.071
N	2.00	0.343	1.280	0.822	0.166

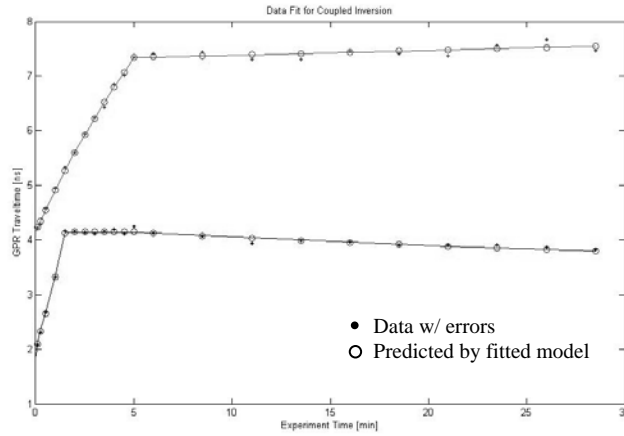


Figure 13: Fit of the GPR traveltime data using the coupled inversion.

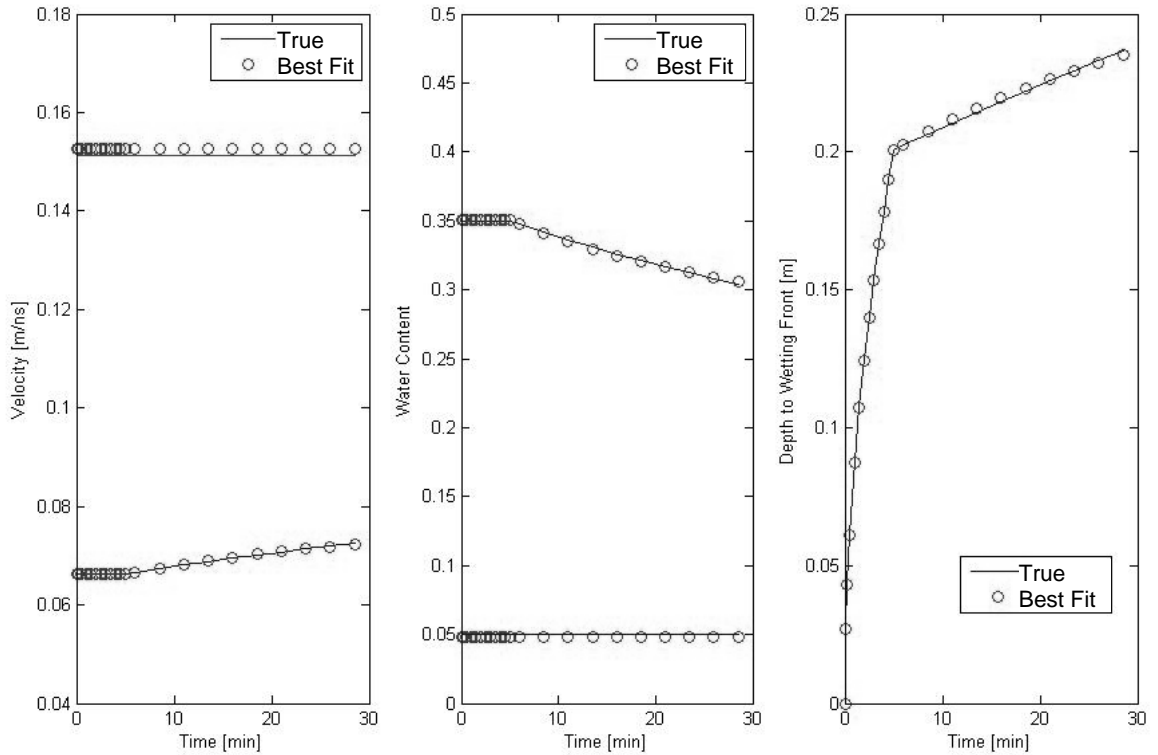


Figure 14: Predicted response of the hydrologic model calibrated using coupled inversion: (a) velocity above and below the wetting front, (b) water content above and below the wetting front, (c) depth to the wetting front. Solid lines represent the true modeled response, whereas the open circles show the water content and wetting front depth predicted by the calibrated hydrologic model using the best fit (i.e., mean) parameters from Table 3.

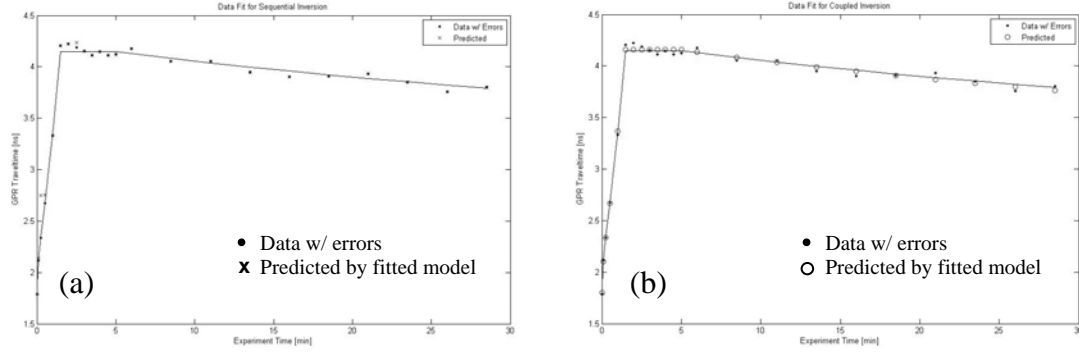


Figure 15: Fit of the ground wave traveltimes data using the (a) sequential and (b) coupled inversion.

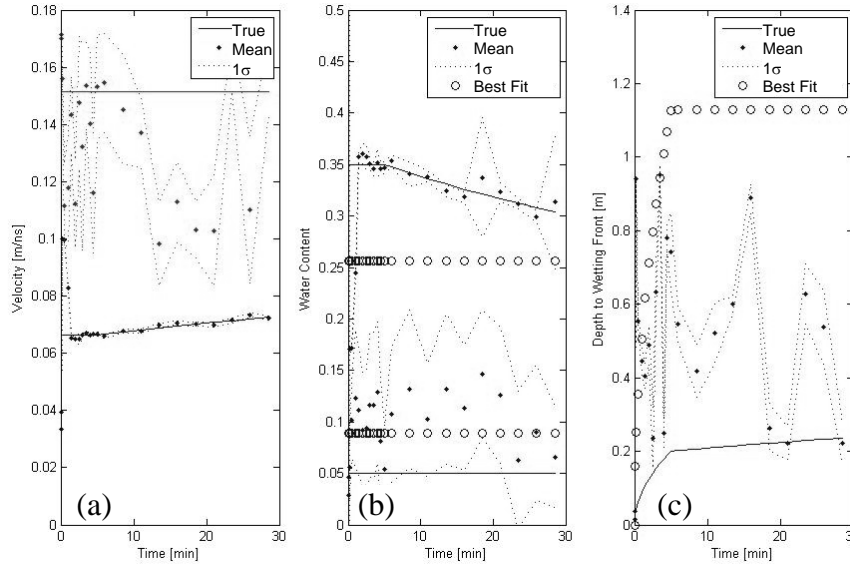


Figure 16: Sequential estimates of model parameters – (a) velocity above and below the wetting front, (b) water content above and below the wetting front, (c) depth to the wetting front.

Dots represent the mean of all parameter sets accepted using the Metropolis-Hastings algorithm and dashed lines represent 1 standard deviation. Open circles show the water content and wetting front depth predicted by the hydrologic parameter using the best fit (i.e., mean) parameters from Table 4. Solid lines show the true model response.

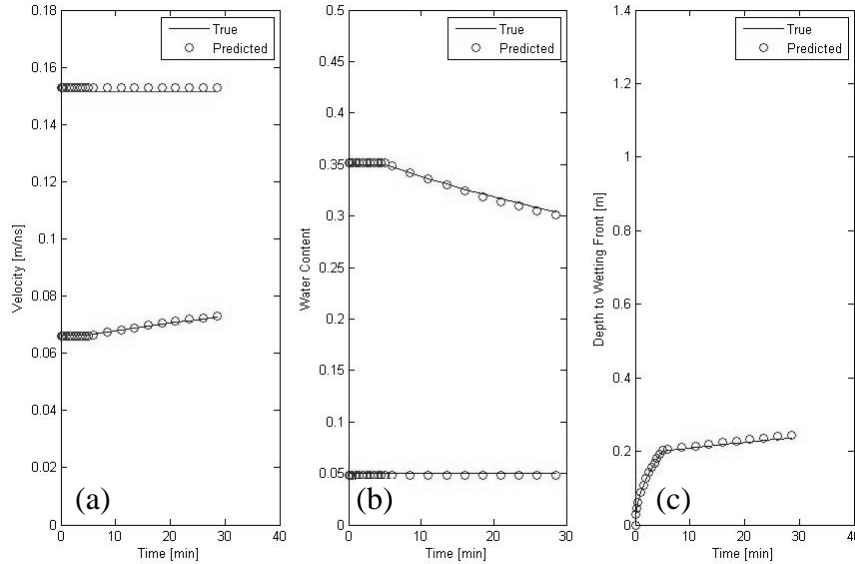


Figure 17: Predicted response of the hydrologic model calibrated using coupled inversion:

(a) velocity above and below the wetting front, (b) water content above and below the wetting front, (c) depth to the wetting front. Solid lines represent the true modeled response, whereas the open circles show the water content and wetting front depth predicted by the calibrated hydrologic model using the best fit (i.e., mean) parameters from Table 4.

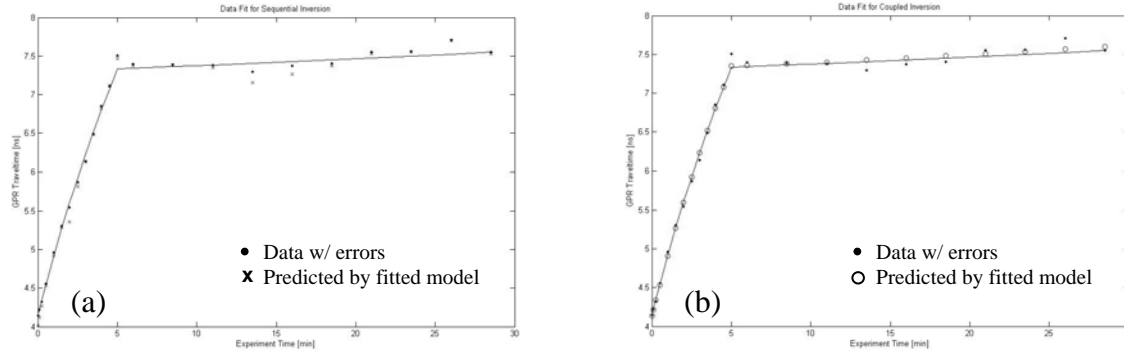


Figure 18: Fit of the traveltime for the wetting front reflection using the (a) sequential and (b) coupled inversion.

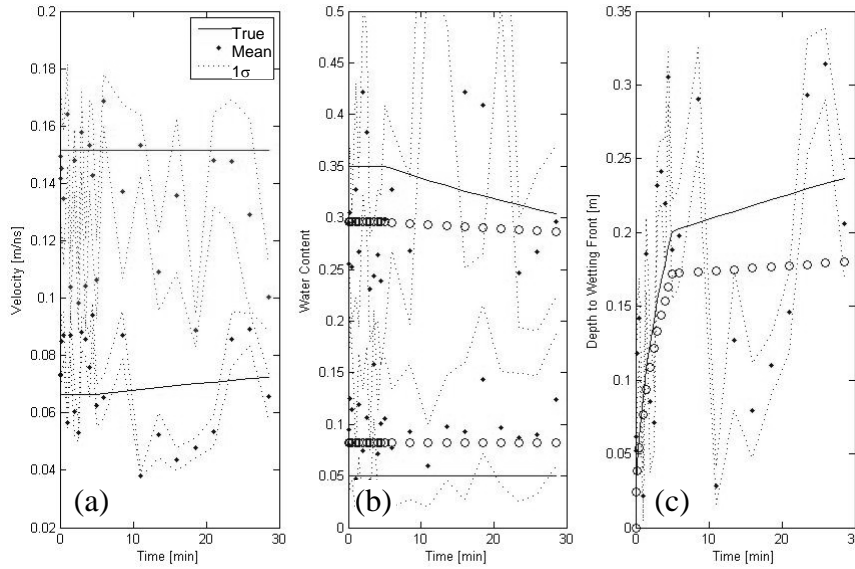


Figure 19: Sequential estimates of model parameters – (a) velocity above and below the wetting front, (b) water content above and below the wetting front, (c) depth to the wetting front.

Dots represent the mean of all parameter sets accepted using the Metropolis-Hastings algorithm and dashed lines represent 1 standard deviation. Open circles show the water content and wetting front depth predicted by the hydrologic parameter using the best fit (i.e., mean) parameters from Table 5. Solid lines show the true model response.

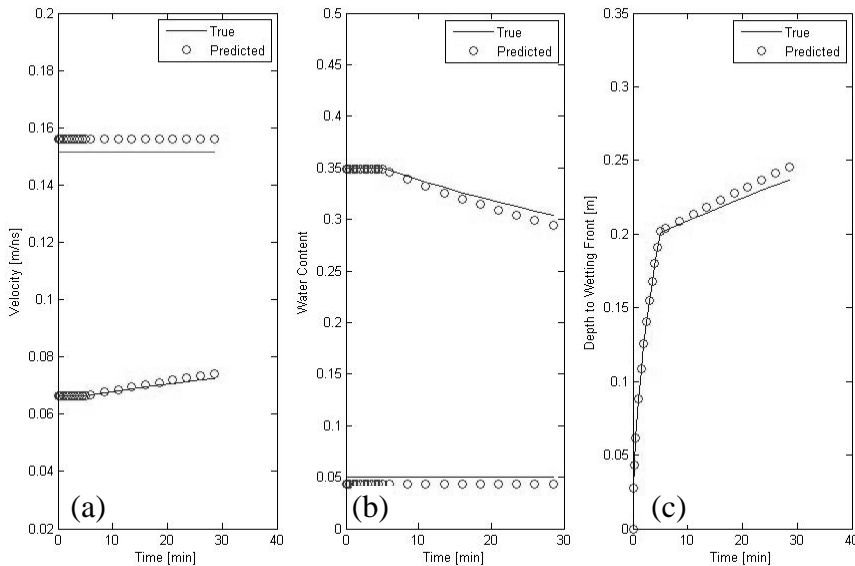


Figure 20: Predicted response of the hydrologic model calibrated using coupled inversion:

(a) velocity above and below the wetting front, (b) water content above and below the wetting front, (c) depth to the wetting front. Solid lines represent the true modeled response, whereas the open circles show the water content and wetting front depth predicted by the calibrated hydrologic model using the best fit (i.e., mean) parameters from Table 5.

The results of the sequential and coupled inversions using only traveltimes for the reflection from the wetting front are shown in Figures 18-20. In this case, there is a strong tradeoff between the velocity above the wetting front and the depth to the wetting front – many combinations of velocity and depth can result in the same traveltime. This fact is evident in the sequential results, where there is a very high correlation between the velocity above the wetting front (Figure 19a, lower lines) and wetting front depth (Figure 19c). Although the sequential inversion converged to parameter reasonable parameter estimates in this case, the highest level of uncertainty was also achieved indicating the reduced degree of constraint of the model.

3.1.4 Conclusions

The coupled inversion scheme was shown to provide better estimates of hydrologic model parameters compared to the sequential approach. Particularly important was the ability of the coupled approach to provide accurate parameter estimates even under limited data constraint. This result suggests that the coupled inversion approach regularizes the inverse problem using the underlying physics driving flow. Overall, the coupled approach is likely to provide better results than sequential inversion, but due to the regularizing role the hydrologic model plays in the inversion, further effort should be made to investigate the impact of conceptual errors in the hydrologic model on the parameter estimates.

3.2 Laboratory-Scale Study of GPR Response to Infiltration

The second part of the study investigated the actual response of GPR to infiltration events. The objectives of this work were to evaluate if strong signal responses could be observed from hydrologically related arrivals (i.e., ground wave and wetting front reflections). This section also describes a new approach to the analysis of GPR data developed through the course of this research.

3.2.1 Experimental Methods

The goal of this study was to generate a uniform vertical flow field over the region that monitored by GPR. The experiments were performed in tanks filled with homogeneous, medium grained commercial sand obtained from CEMEX USA (e.g., Figure 21). Gravel was placed under the sand to allow for drainage. The flux of water applied at the top of the tank was controlled using a variable rate peristaltic pump (Preston Monostat, Cole-Parmer) calibrated for a custom drip irrigation system with outlets created on a 1cm x 1cm grid over the entire tank surface by using a syringe to puncture holes in 6mm Tygon tubing. Figure 22 illustrates the irrigation system. Calibration experiments showed that spatially uniform flow could be approximately achieved using the system. Capacitance probes (EC5, Decagon Devices, Inc.) were distributed at two depths and at seven different locations in the tank (shown in Figure 23) to monitor the uniformity of changes in near-surface water content and the arrival of the wetting front at the bottom of the tank. Tensiometers were also included to monitor pressure in

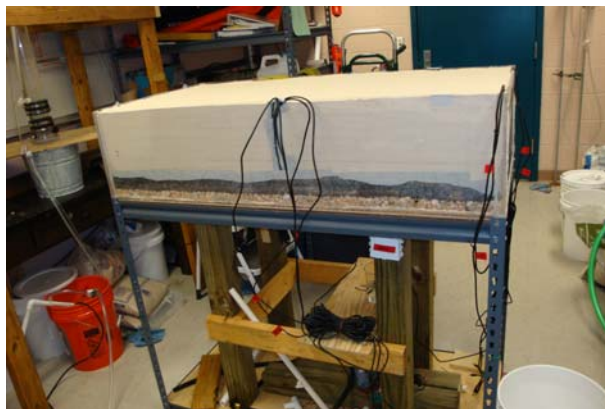


Figure 21: Example of the packed sand boxes used for the infiltration tests.

some experiments, but are not reported on here as technical problems were experienced in obtaining reliable data.



Figure 21: Illustration of the irrigation system with the GPR antennas resting on the tubing.

The GPR system used in this study was a Sensors and Software pulseEKKO 1000 with 450 and 900 MHz antennas. The antennas were placed in the center of the tank directly on top of the tubing used for water application. The antenna separation was 37cm, as measured from the centers of the transmitter and receiver antenna. The antennas were not moved at any point during the experiments. GPR traces were collected approximately every 3 seconds throughout the experiment. No processing was performed on the GPR data.

Independent measurements of soil hydraulic properties were performed for samples of the sand used to pack the flow tank. The saturated hydraulic conductivity (K_s) of the sand was measured using a constant head permeameter. The saturated water content (θ_s) was obtained gravimetrically by oven drying a saturated sample of known volume. The water retention curve was determined using the hanging column method, which was fitted using the model of van Genuchten

[1980] to estimate the residual water content (θ_r) and parameters α and n . The resulting parameter values from these measurements are given in Table 6.

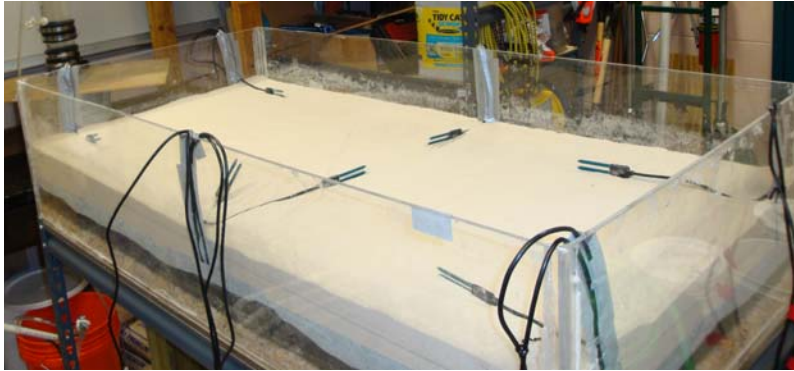


Figure 23: Illustration of the moisture probe distribution used to monitor uniformity of flow across the sand tanks. One probe was located in each quadrant of the tank and three probes were located in the center of the tank to identify non-uniform flow.

Table 6: Measured hydrologic properties of the sand used in the flow experiments.

θ_r	θ_s	α^* [cm ⁻¹]	n^*	K_s [cm/min]
0.041	0.385	0.033	6.26	1.43

*a and n are fitting parameters from the van Genuchten water retention model

Initial experiments while the system was being designed and tested were performed using the small flow tank shown in Figure 21, which was only 30cm deep. Because we dried the sand between experiments, the use of the smaller tank allowed us to cycle between wet and dry sand during the testing phase of the project. Figure 24 is included here to show the reason why a larger tank was used in later experiments that we report on in the results section and also to illustrate the impacts that near-surface heterogeneity may have on GPR data. In this data, the tank depth is too small to allow for the separation of arrivals resulting from the movement of the wetting front versus the reflection from the bottom of the tank. Therefore, it is not possible to uniquely identify the response of the wetting front. For example, it is not possible to pick the traveltime for the reflection from the wetting front that would be needed to perform the type of model calibration discussed in the previous section of this report.

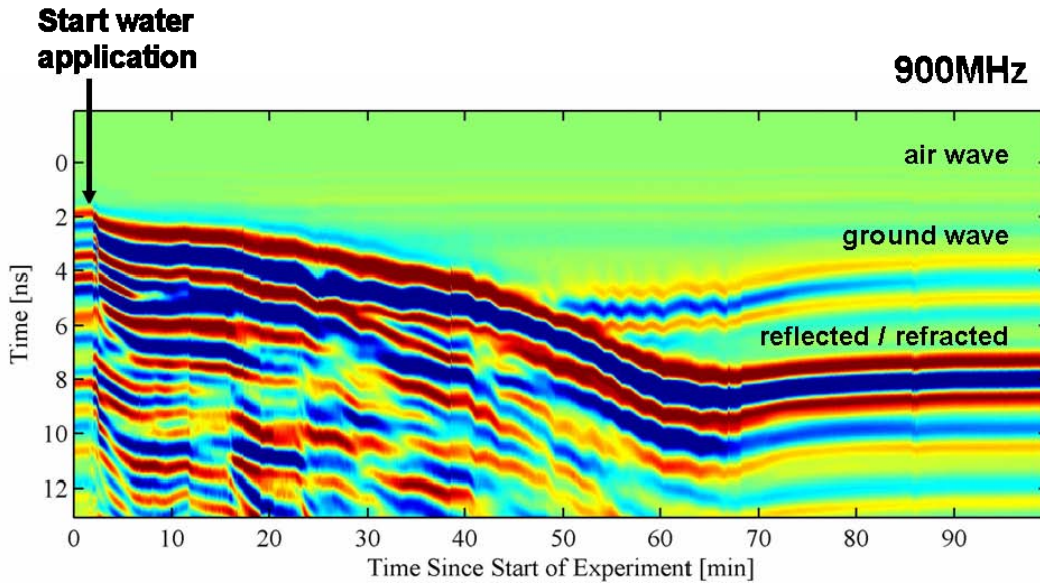


Figure 24: Example of GPR data collected in a small tank of 30cm depth. Note that it is not possible to identify unique arrivals related to the wetting front in the tank from those produced by the interface at the bottom of the tank. This figure illustrates why a deep tank is required in this research.

The main experiments were conducted in a flow tank packed with sand to a depth of 50cm, under which 16cm of gravel was placed to ensure good drainage. During the experiments, the rate of flow was changed over time to create both transient and pseudo-steady state moisture conditions in the tank. Capacitance probes were distributed at depths of 5.5 and 45 cm at the same seven spatial locations in the tank as shown in Figure 23.

3.2.2 Experimental Results

The results for the flow experiment monitored using 900MHz and 450MHz GPR antennas are shown in Figures 25 and 26, respectively. The experiment-specific schedule for the applied flux to the tank surface is given in Table 7. A variety of arrivals can be clearly identified in the data, including the air wave, ground wave, reflections from two different wetting fronts, and a strong reflection at the boundary between sand and gravel. Coherent noise at late times is likely the result of reflections from the sides of the tank and reflection multiples.

Table 7: Schedule of applied flux for 900MHz experiment; experiment ended after 156.5 minutes.

Experiment Time [min]	0.0	4.0	42.0	42.3	64.9	70.7	77.5	77.9	90.0
Applied Flux [cm/hr]	0	2.1	0	10	0	10	0	21	0
Experiment Time [min]	95.0	110.3	122.7	131.3	122.7	131.3	136.2	142.8	156.5
Applied Flux [cm/hr]	21	0	41	0	41	0	41	0	END

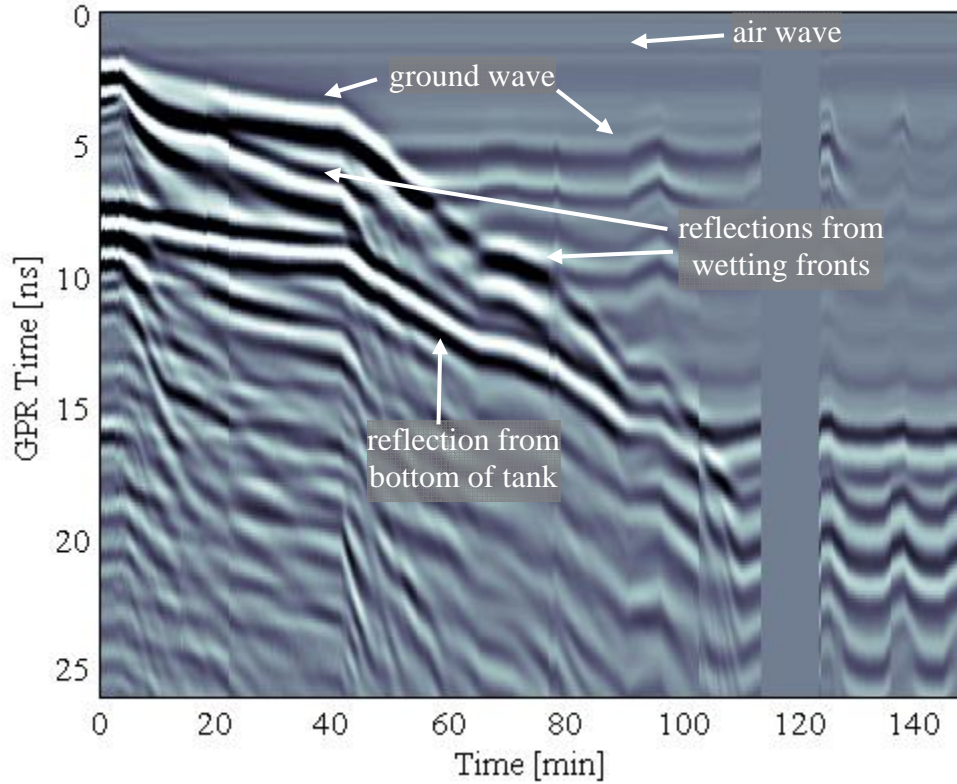


Figure 24: Interpreted 900MHz GPR data during an infiltration experiment.

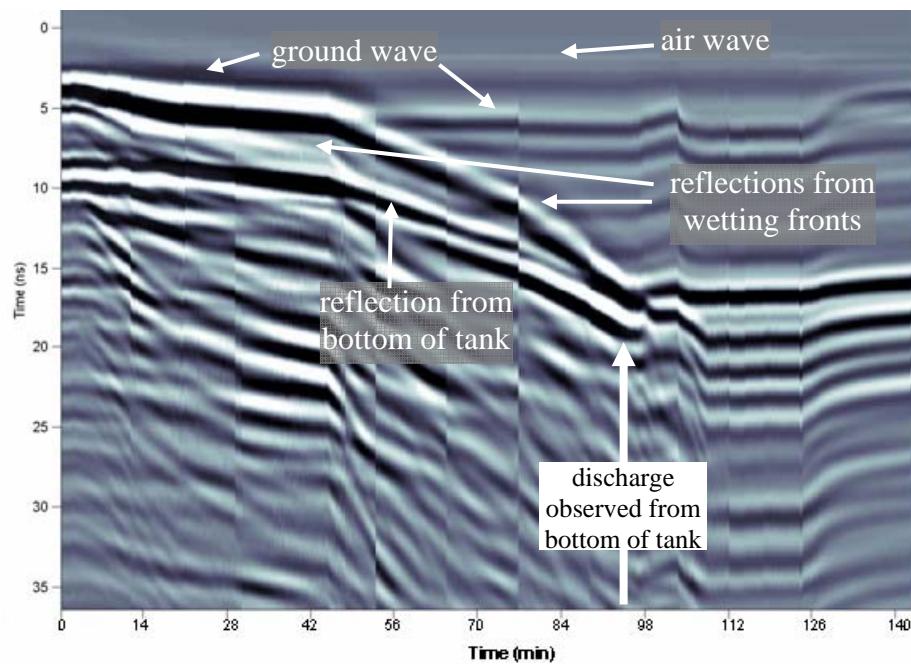


Figure 25: Interpreted 450MHz GPR data during an infiltration experiment.

Table 8: Schedule of applied flux for 450MHz experiment.

Experiment Time [min]	0.0	2.0	40.0	68.0	88.0	95.0	128.0	142.0
Applied Flux [cm/hr]	0.0	2.4	10.9	21.7	0.0	38.8	0.0	END

There are several significant differences in the results for the two frequencies. Perhaps most importantly, the reflection from the initial wetting front is obvious in the 900MHz data, whereas it is difficult to identify in the 450MHz data because of interference between it, the ground wave and the reflection from the bottom of the tank. Another difference is in the response of the ground wave arrival time. There is a much greater change in the ground wave traveltime at early times during the experiment for the 900MHz data than the 450MHz data. This type of behavior is consistent with the difference in the sampling depth of the ground wave for the two frequencies; at lower frequency the sampling depth is larger resulting in a less pronounced change in apparent velocity at early times. These results suggest that all GPR arrivals are sensitive to infiltration, but that the frequency used in a monitoring experiment should be dependent on the scale of heterogeneity in the subsurface and the length of time of the experiment (i.e., maximum depth of the wetting front).

3.2.3 Numerical Validation of Experimental Results

To evaluate the empirical data, simulations of the GPR response were performed using the flow model HYDRUS-1D [Simunek et al., 2008] and a MATLAB based 2D GPR simulator created by Irving and Knight [2006]. The flow was simulated using the known boundary conditions of the experiment, i.e., the applied fluxes given in Table 7 at the upper boundary and a seepage face condition on the lower boundary. The independently measured hydraulic properties of the sand in Table 6 were used in the simulations.

A comparison of the observed and simulated GPR response is given in Figure 26. The match between the simulated GPR response and the observed data is excellent given that the model prediction is based on independent samples and not calibrated to the observed response. The ground wave, second wetting front, and bottom reflection are all clearly visible in the data. An exception is the apparent absence of the reflection from the first wetting front. This arrival can be found in the simulated data, but has much lower amplitude than in the empirical response so is difficult to identify in the Figure. The patterns observed for the shifts in the ground wave arrival also show excellent qualitative agreement with both the observed and simulated average water content between 4-7cm depth; note that the average water content was used to represent the support volume of the capacitance sensors. The traveltime for each of the main arrivals in the simulated data are plotted overtop of the empirical data in Figure 26a to provide a direct comparison between the results. It is apparent that there is generally a good match except during the period between 50-75 minutes where the simulated traveltimes are less than the observed response. The discrepancy between the observed and simulated water content can be explained by the underestimation of observed water content by the simulations in the near surface during this period (Figure 26c).

An important outcome of the empirical and numerical results is the observation of hydrologic trajectories in continuously monitored GPR data during infiltration events. For example, the ground wave arrival follows a complex, but well defined path throughout the experiment that can be reproduced using existing numerical models. The ability to reproduce complex patterns in the GPR data through time suggests that such patterns may be useful tools for hydrologic characterization.

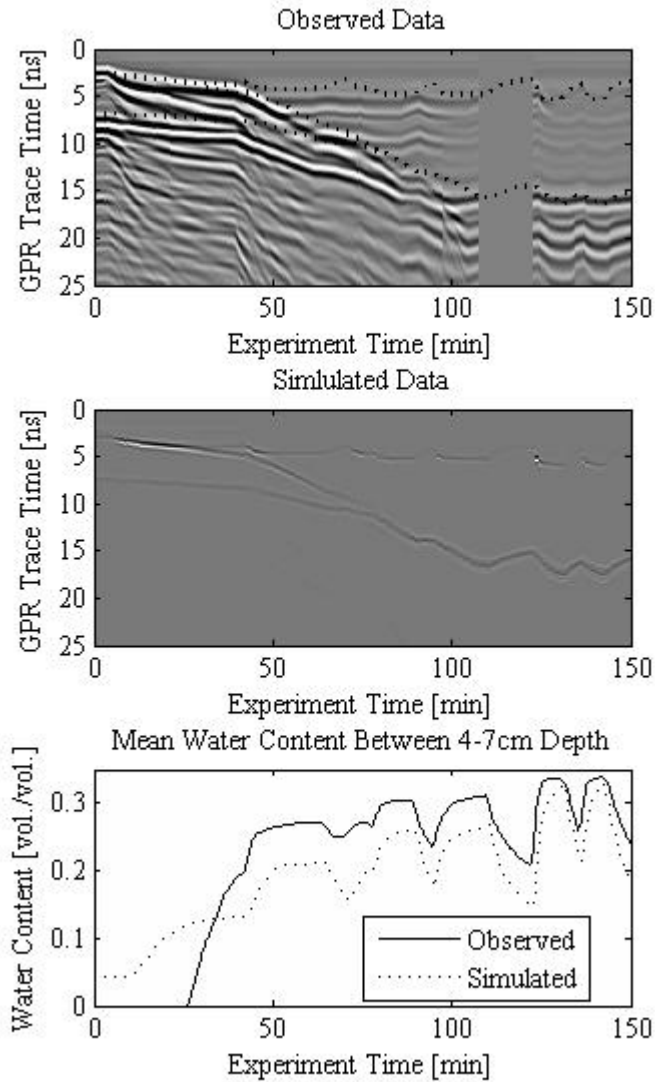


Figure 26: (a) Observed GPR response during infiltration event, dotted line shows comparison to arrival times in simulated data; (b) simulated GPR response based on lab measurements of hydraulic parameters, (c) average observed and simulated water content between 4-7cm depth, (d) water application schedule.

3.2.4 Coherency analysis of GPR data using hydrologic trajectories

The observed temporal trajectories observed in the GPR response to infiltration are reminiscent of the spatial trajectories observed in multi-offset data. Multi-offset surveying, such as traditional central midpoint (CMP) and wide angle reflection and refraction (WARR) surveys, are well known methods for estimating water content variations with depth [Greaves et al., 1996; van Overmeeren et al., 1997; Garambois et al., 2002]. Processing of multi-offset data is typically performed by applying normal moveout corrections to determine the one dimensional velocity structure of the subsurface [e.g., Yilmaz, 1987]. This is possible because the change in reflector traveltimes with antenna offset in a common midpoint gather follows a hyperbolic trajectory that is directly dependent on RMS velocity (Figure 2). Neidell and Taner [1971] discussed the use of coherency measures, such as semblance, calculated along these moveout trajectories as a means for determining velocity in seismic data and the approach has since also become a standard method for velocity estimation in GPR workflows [Fisher et al., 1992; Neal, 2004]. Water

content can be calculated from interval velocities in environments with low electrical conductivity when an appropriate rock physics relationship is available [Greaves et al., 1996].

Analogous to the normal moveout approach to estimating velocity, I suggest that the temporal trajectories in constant offset GPR data can be used to identify unsaturated flow parameters. Just as in standard semblance analysis to estimate velocity, I propose that it is possible to calculate the coherency of the GPR signal along hydrologic trajectories that are dependent on hydrologic variables. This approach to analyzing GPR data would provide a unique means for identifying these variables and would be a particularly valuable tool if it could be performed by defining the trajectories using methods with low computational cost.

Predicting the GPR traveltimes for different arrivals, e.g., ground wave, reflections, refractions, etc., is straightforward for models with sharp wetting fronts. In this case, the same type of ray calculations performed in Section 3.1 can be used to determine the trajectories as function of the hydrologic parameters. For each set of hydrologic parameters, a window of data along the trace is extracted and realigned so that a measure of coherency between the traces, such as semblance, can be calculated (Figure 27).

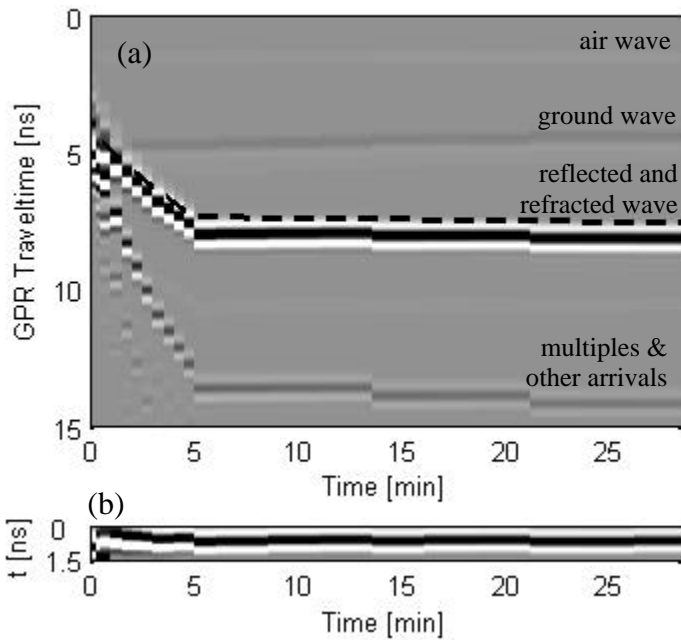


Figure 27: (a) Synthetic GPR data for the infiltration example using the Philip model. The dashed line shows the semblance analysis trajectory for the wetting front reflection calculated using ray theory.

(b) GPR data extracted in a 1.5ns window along the wetting front reflection trajectory and realigned.

To explore the use of semblance calculations for different types of arrivals (i.e., ground wave, wetting front reflection, and wetting front refraction), a sensitivity analysis was performed for each of the hydrologic variables of the Philips infiltration and rectangular drainage model described in Section 3.1.2. The results of the sensitivity analysis are shown in Figure 28 for the parameter set given in Table 1 and synthetic GPR data in Figure 27. The results show that when all three arrivals are used in the calculation the semblance reaches a well-defined maximum at the true parameter values, except for the N parameter which has a poorly defined maximum consistent with the results of the MCMC analyses in Section 3.1. Taken individually, however, the semblance maximum was sometimes poorly defined or was biased toward incorrect values. This was particularly true for the ground wave results. This outcome is not consistent with the

MCMC results discussed earlier where the ground wave was able to provide good constraint on the hydrologic model parameters. This indicates that the sensitivity of the semblance approach is slightly different than calibration by traveltimes.

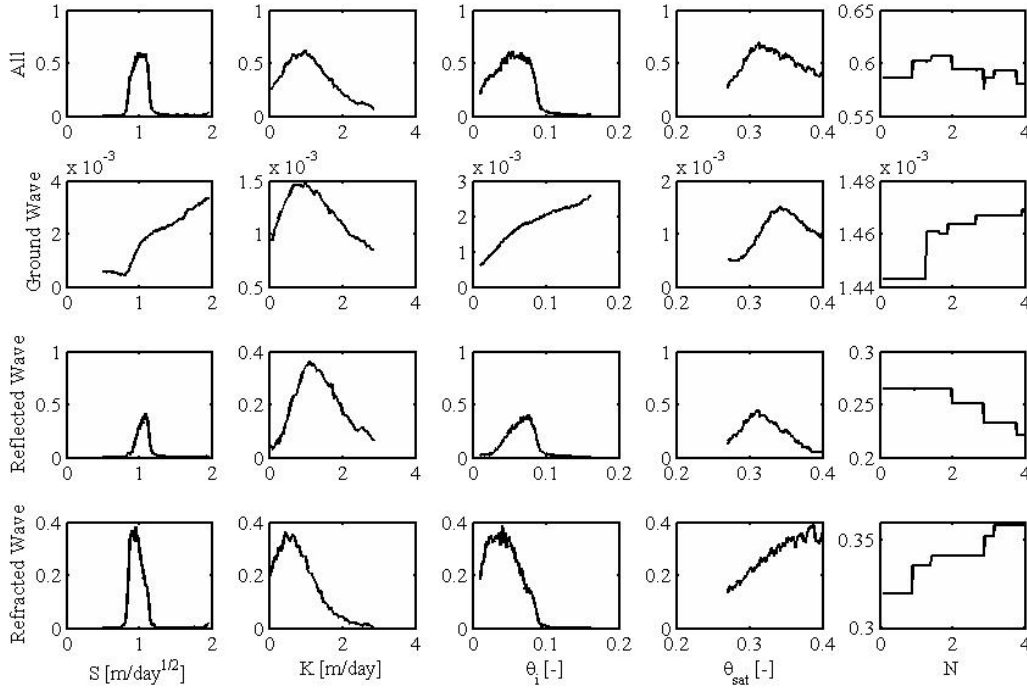


Figure 28: Sensitivity analysis for semblance as a function of parameters of the Philip infiltration and rectangular distribution model. The bottom three rows show results for the ground wave, reflected wave from the wetting front, and refracted wave, respectively. The top row shows results by summing the semblance from all three arrivals. When all three arrivals are combined, the maximum semblance occurs at the true parameter values.

In cases where more complex flow occurs, as in the multi-flux infiltration test performed in the lab (Figure 26), more complicated hydrologic models must be used. In this case, the lack of a well-defined wetting front in the model may prevent the calculation of arrival times using the approach described above. An alternate method was developed in this research that is based only on analysis of simulated water contents derived from a numerical model. First, the water contents simulated over time are converted to dielectric constants. The dielectric constants are used to calculate profiles of reflection coefficients and velocity variations with depth. The reflection coefficients are indicative of areas where reflections are likely to occur, i.e., strong signal returns would be expected in the GPR data. The velocities are then used to remap the reflection coefficients from depth profiles to profiles in terms of GPR arrival times. The result is then filtered to select only the regions with the strongest reflection coefficients, which gives a map of trajectories (as in Figure 27). The trajectories are then used to extract windows out windows from the observed GPR data for coherency analysis. Note that this approach is based on reflection coefficients and therefore only provides trajectories related to reflections. It is therefore most suitable for cases where hydrologic changes dominate the GPR response. A sensitivity analysis for the multi-flux infiltration experiment (Figure 26) is given in Figure 29. In this case the total signal power in the window was used as the coherency measure instead of

semblance. The results indicate that excellent constraint of the parameters for the Mualem-van Genuchten model for the unsaturated flow parameters can be achieved, except for the n parameter.

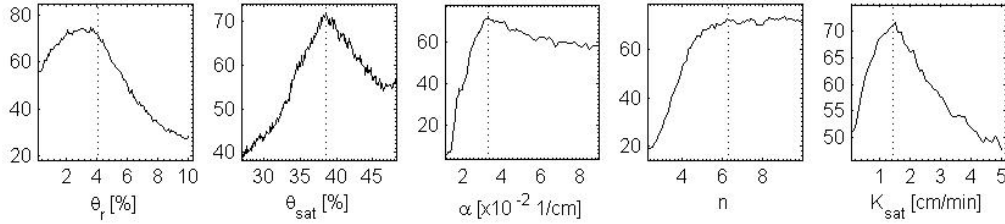


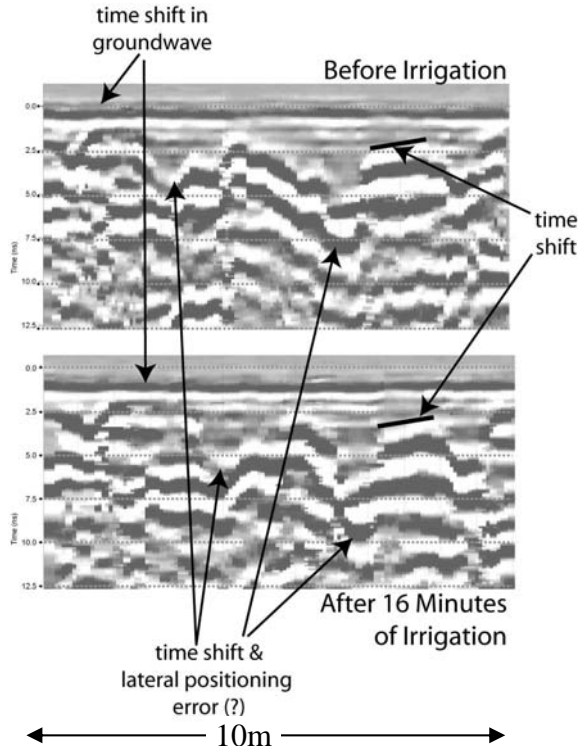
Figure 29: Sensitivity of total signal power along trajectories of GPR data as a function of hydrologic parameters for the multi-flux infiltration test. Note the maximum power occurs at the true parameter value (shown with a dashed line).

The sensitivity analyses presented here suggest that the coherency approach to estimating hydrologic parameters has excellent potential for the hydraulic analysis of GPR data.

3.3 Field-Scale Study of GPR Response to Infiltration

Field-scale experiments have also been conducted to perform an exploratory investigation of GPR response to infiltration in heterogeneous soils. In these experiments, we used a sprinkler system to irrigate an approximately 10m x 5m region of a silty-sand soil. Soil moisture probes were installed at multiple depths to monitor the movement of the wetting front. The rate of water application over the site was monitored through time using a tipping bucket rain gauge. GPR was profiled across the site at multiple times during the infiltration experiment. The GPR was profiled between fixed stations, but due to an inability to integrate in real-time positioning information with our current GPR system and the discontinuation of odometer wheel triggering devices by the manufacturer of our radar, we were unable to precisely position the data. We found that careful manual positioning at fixed stations was a poor solution to the positioning problem because for each GPR profile to be collected the sprinklers had to be stopped. As a faster alternative, we attempted to consistently move the antennas at a constant velocity across the site. This approach introduced the potential for positioning errors. Despite the possible

Figure 30: Two 10m transects of GPR data collected during a field infiltration experiment. The upper image shows the data collected prior to the start of the irrigation sprinklers. The bottom image shows the same transect profiled after 16 minutes of water application to the site. Note the shift in the groundwave and other reflections is a result of increased water content (decreased wave velocity) of the soils.



positioning errors, Figure 4c illustrates the shift in the arrival time of the groundwave and different reflections across the site as a result of the infiltration event. In some areas, there is a change in the character of the GPR image that is likely to be related to the infiltration (i.e., shifts in reflections to later times). These changes are not uniformly distributed over the site and it is currently unclear whether this is an effect resulting from heterogeneous water infiltration or errors in positioning the antennas. This experience underscores the need for improved positioning capabilities for this type of field research.

In addition to the collection of GPR data, approximately 30 soil samples were collected during the project to characterize soil variability. Because these soils drain at relatively low pressure, we investigated a method for characterizing the soil retention curve suitable for use with large numbers of samples. Each sample was packed in a ~50cm column and then placed vertically with one end in a water reservoir. The samples were allowed to equilibrate such that at equilibrium the flux in the column is zero and the pressure distribution is equal to the elevation along the column. The columns were then sampled along their length and the water content was measured for each sample, yielding water content measurements at known pressures. While the technique showed promise, problems with packing and sampling the columns put into question whether the results are reliable. Additional analysis and repeat tests are required to fully evaluate the results.

4. Project Conclusions

This short term research project has demonstrated the potential of GPR for constraining the parameters of unsaturated flow models using the coupled approach to hydrogeophysical estimation. This is particularly true when GPR data contain insufficient information to independently constrain the hydrologic model. In this case, the coupled approach allows the hydrologic model to regularize the inversion and produce reliable estimates of hydrologic parameters. Stochastic calibration of models using traveltime data was shown to be effective for simple flow scenarios. Coherency analysis along hydrologic trajectories, a new methodology that was developed as a result of this research, shows promise for identifying hydrologic model parameters for more complicated flow scenarios. The behavior of the ground wave during infiltration was one particular point of interest in this research. It was shown that the ground wave response is sensitive to flow processes and can be used to calibrate hydrologic models. This research also suggests, however, that reflection data provide additional information on the rate of flow and can be readily included in model calibration algorithms. Therefore, it is recommended that all GPR arrivals be used to calibrate hydrologic models when possible.